



Uncovering Inundation Hotspots through a Normalized Flood Severity Index: Urban Flood Modelling Based on Open-Access Data in Ho Chi Minh City, Vietnam

5 Mazen Hoballah Jalloul¹, Leon Scheiber¹, Christian Jordan¹, Jan Visscher¹, Hong Quan Nguyen^{2,3} and
Torsten Schlurmann¹

¹Ludwig-Franzius-Institute of Hydraulic, Estuarine and Coastal Engineering, Leibniz University of Hannover, D-30167 Hannover, Germany

²Institute for Circular Economy Development, Vietnam National University – Ho Chi Minh City, 700000 Ho Chi Minh City, Vietnam

10 ³Institute for Environment and Resources, Vietnam National University – Ho Chi Minh City, 700000 Ho Chi Minh City, Vietnam

Correspondence to: Leon Scheiber (scheiber@lufi.uni-hannover.de)

15 **Abstract.** Hydro-numerical models offer an increasingly important tool to determine the adequacy and evaluate the effectiveness of potential flood protection measures. However, a significant obstacle in setting up hydro-numerical and associated flood damage models is the tedious and oftentimes prohibitively costly process of acquiring reliable input data, which particularly applies to coastal megacities in developing countries and emerging economies. To address this problem, this paper takes the example of Ho Chi Minh City, Vietnam, and proposes a new and comprehensive methodology for
20 acquiring, processing, and applying the necessary open-access data (topography, bathymetry, tidal, river flow, and precipitation time series) to set up an urban surface run-off model. As a key novelty of the paper, a normalized flood severity index (NFSI) that combines flood depth and duration is proposed. The index serves as an indicator that helps uncover urban inundation hotspots with severe damage potential, drawing attention to specific districts or boroughs with special adaptation needs or emergency response measures. The approach is validated by a comparison with more than 300 locally reported flood samples,
25 which correspond to NFSI-processed inundation hotspots in over 73 % of all cases. These findings corroborate the robustness of the proposed index, which may significantly enhance the interpretation and trustworthiness of hydro-numerical assessments in the future. The proposed approach and developed indicators are generic and may be replicated and adopted in other coastal megacities.

Keywords: urban flooding, disaster risk, numerical modelling, surface runoff model, Ho Chi Minh City, Southeast Asia



30 **1 Introduction**

With more than half a million deaths between 1980 and 2009 and nearly three billion people affected, flood events are doubtlessly the most common and impactful natural disasters worldwide (Doocy et al., 2013; Hong et al., 2018; Hallegatte et al., 2013). Climate change is expected to significantly amplify the probability of extreme flood events during the next decade, especially in Southeast Asia, where the number of coastal cities is disproportionately high (Hanson et al., 2011). This trend is especially worrisome since half of the people living in cities of at least 100,000 inhabitants are not farther than 100 km from the coast (Barragán and Andrés, 2015). Some of these cities are also accompanied by uncontrolled urban sprawl (Kontgis et al., 2014; Phung, 2016; Storch, 2011; Huong and Pathirana, 2013), which exacerbates the risk of disaster-induced damages due to the combination of increased exposure and vulnerability (IPCC, 2022). To respond to this problem, local decision-makers require a sound understanding of the complex inter-play of underlying natural processes that dictate the feasibility and effectiveness of possible adaptation strategies (Beven, 2011; C.R. Thorne et al., 2015). This knowledge is typically enriched through the application of hydro-numerical models. These, in turn, rely on information about prevailing environmental constraints, such as the topography and hydro-meteorological conditions (Quan et al., 2020; Nkwunonwo et al., 2020; Ozdemir et al., 2013; Kim et al., 2019).

With respect to Southeast Asia, many national institutions still refrain from making this crucial input data available for various (technical or political) reasons (Kim et al., 2018; Hamel and Tan, 2021; Liu et al., 2020), which complicates numerical studies, especially for independent parties. However, relevant information is increasingly published by international researchers, either in connection with scientific articles or on independent databases (Di Baldassarre and Uhlenbrook, 2012; René et al., 2014). An increasing number of online media articles, open climate models, and code repositories further add to this trend. Accordingly, several studies have recently discussed the possibility and implications of deriving modeling inputs from open-access data sources. This includes local hydro- and meteorological boundary conditions, such as rainfall intensities (Zhao et al., 2021) and sea level rise scenarios (Brown et al., 2016), as well as topographic elevation models (Schellekens et al., 2014; Sanders, 2007). In addition, the expansion of social media applications continuously improves the potential to validate the results of urban flood models (Wang et al. 2018; Feng et al., 2020). Some efforts have been made to build models based in part on open-access data in regions of the world where data is scarce (Trinh and Molkenhain, 2021; Pandya et al., 2021; Ekeuwei and Blackburn, 2020; Mehta et al., 2022). However, to this date, no efforts have been made to create a complete urban surface runoff model, which is exclusively built on freely available data, although this would be a worthwhile target to illustrate the necessity as well as the benefits of comprehensive data accessibility. Furthermore, no efforts have been made to develop a simple flood severity index that combines flood depth as well as duration, both of which have significant impact (Rättich et al., 2020), to deliver a more complete picture of the potential damage that flooding can cause in the absence of extensive data necessary for a flood damage model.

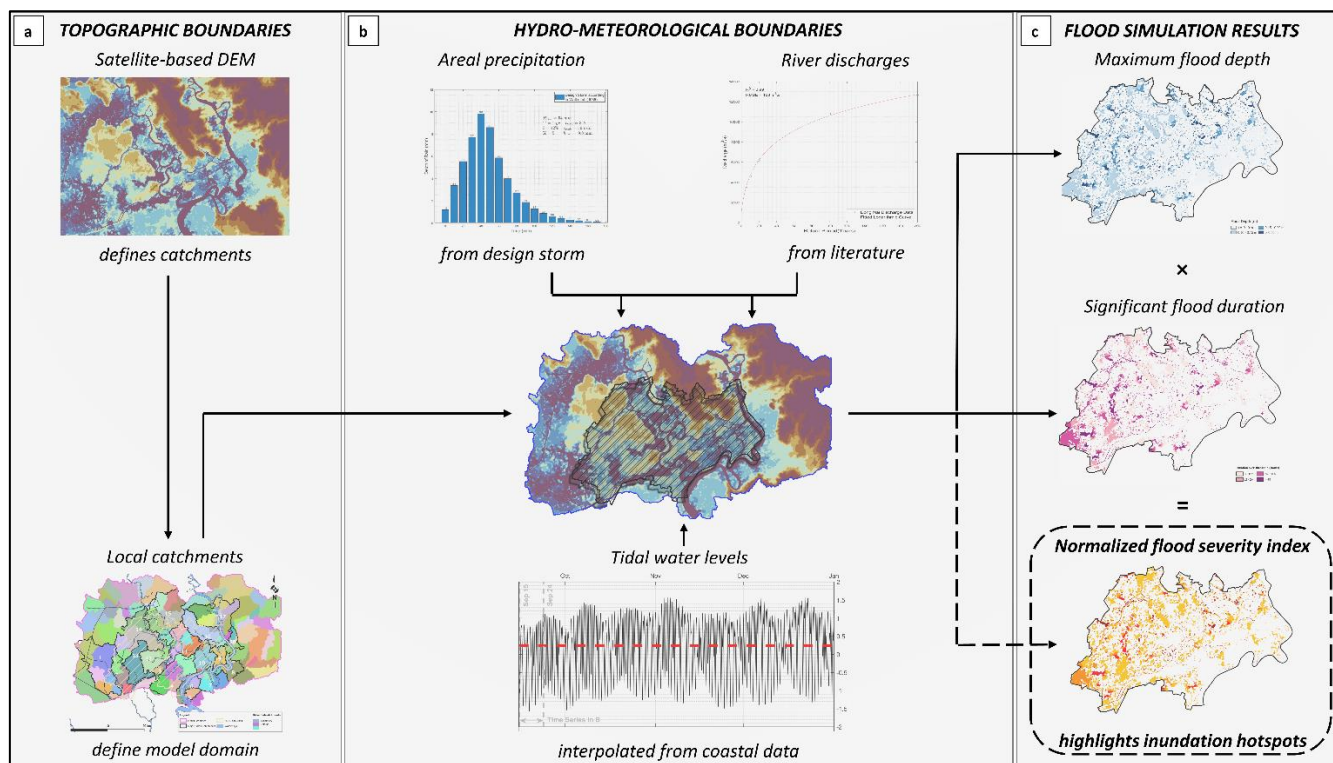
Studying the metropolitan area of Ho Chi Minh City (HCMC), Vietnam, the present paper explores if and by what means an urban flood model can be developed without acquiring any exclusive spatial or hydro-meteorological data. It focuses on the



methodological steps required to derive trustworthy boundary conditions from cross-referencing of several freely accessible and reliable sources. These include open-access satellite imagery, governmental and scientific databases as well as data and information from open-access journal articles. Secondly, the paper introduces a new perspective on flood intensity by proposing a normalized index, which integrates simulated flood depth and duration to facilitate an estimation of damage potential. Both approaches are finally validated by contrasting the individual model components and resulting inundation hotspots with conventionally acquired information and data from local partners. It, therefore, proves the developed concept, accounts for the feasibility of the primary objective, and legitimates the call for open-access data and open science (Miedema, 2022) in the field of urban flood modeling on a worldwide scale.

2 Materials and Methods

There are generally two essential inputs that a hydro-numerical model needs to produce reliable results. These are elevation data including the hydraulic roughness and the model domain based on topographic boundaries (Figure 1 (a)), and hydro-meteorological data, such as tidal water levels, river discharge, and precipitation data depending on the investigated environment (Figure 1 (b)). The ensuing simulation results can be interpreted using model outputs like flood depth and duration, which can be combined into flood severity (Figure 1 (c)). The acquisition, processing, and implementation of the input as well as the processing of the output require further methodological steps, which will be discussed in the following subsections. Regarding data acquisition, special attention needs to be given to the source, since it dictates the reliability and completeness of the data. Generally, terrain data, as well as hydro-meteorological data, have similar sources and the search priority follows the same path, with official sources at the top, followed by global repositories, peer-reviewed literature, *grey* literature (i.e. publicly available reports and assessments), and finally regional and global models. This workflow will be demonstrated in the following sections by the HEC-RAS 2D (a capable and freely available program based on the 2D shallow water equations) model built for the metropolitan region of HCMC.



85 **Figure 1: WORK FLOW:** (a) The first panel shows the topographic data from which the local catchments can be determined that
 90 define the final model domain; (b) in the second step, hydro-meteorological time-series are defined, which serve as boundary
 conditions for the numerical model; (c) thirdly, simulation results are presented in terms of maximum flood depth, significant flood
 duration as well as in the integrated form of a normalized flood severity index (NFSI) that is to be defined within this work.
 Topographic data visualized using scientific color maps created by Crameri (2021). All other maps use colors for illustration
 purposes only

2.1 Surface Elevation Data

2.1.1 Topographic Data

For most parts of the world, accurate and reliable data on local topography is hard to acquire without financial efforts. Data
 from high-resolution LiDAR (Light Detection and Ranging) is freely available only for the coastal USA, coastal Australia,
 95 and parts of Europe, but not for the majority of developing countries and emerging economies like Vietnam (Meesuk et al.,
 2015). This is particularly problematic when setting up urban surface runoff models which heavily depend on terrain elevation.
 The only alternative to self-measurements or unvalidated commercial digital elevations models (DEM) (Planet Observer, 2017;
 Takaku and Tadono, 2017; Intermap, 2018) for the rest of the world, both of which are prohibitively costly (Hawker et al.,
 2018), are open-access satellite-based DEMs. An example of such open-access DEMs is the highly popular Shuttle Radar
 100 Topography Mission (SRTM) (Rexer and Hirt, 2014; Jarihani et al., 2015; Sampson et al., 2016; Hu et al., 2017), which was
 acquired in 2000 and covers around 99.7% of the global populated areas (Bright et al., 2011). However, these models have
 substantial vertical errors, and relatively coarse resolutions and, thus, cannot reflect micro-topographic features or



infrastructure developments in relatively flat terrain (Gallien et al., 2011; Chu and Lindenschmidt, 2017). This is also true for urban settings due to a positive bias created by the backscatter of buildings and vegetation (Tighe, M. & Chamberlain, D., 2009; LaLonde et al., 2010; Shortridge and Messina, 2011; Becek, 2014), making them unable to resolve terrain features that actually control flooding extent and its dynamics (Schumann et al., 2014). In fact, the mean error of SRTM can reach up to 3.7 m when compared to LiDAR (Kulp and Strauss, 2019), significantly distorting simulated flood extents for coastal areas under considerable tidal influences. An attempt to rectify these errors was undertaken by Kulp and Strauss (2018), who developed a novel CoastalDEM by using a neural network to perform a nonlinear, non-parametric regression analysis of SRTM errors, suggesting better performance and adequacy in urban environments. Although CoastalDEM provides better elevation accuracy especially in urban settings, its plausibility still needs to be checked for each individual study area. This can be done through the inspection of terrain elevation at key locations which can either be structures (canal banks/dikes/flood protection structures) or locations where flooding is frequently reported (hotspots) all the while taking the elevation data of other satellite-DEMs like ALOS, ASTER, SRTM and COPERNICUS into account. Another issue with the freely available version of CoastalDEM is its resolution of 3 arc seconds, whereas other open access satellite-based DEMs are available in a 1 arc second resolution. A list of available DEM data sets, their resolution, and providing agencies is given in Table 1.

Table 1. A list of freely available DEMs along with their different versions, their issuers and their date of issuance as well as their resolution.

Freely Available Satellite DEMs				
Name	Version	Issuer with Link (Reference)	Publication Date	Horizontal Resolution
SRTM	1	NASA	2004	3-arcsecond
	2.1	(Earth Resources Observation and Science	2005	3-arcsecond
	3	(EROS) Center, 2018)	2013	1-arcsecond
ALOS	1	JAXA	2015	1-arcsecond
	2	(OpenTopography, 2016)	2017	1-arcsecond
	3		2020	1-arcsecond
ASTER	1	NASA/METI	2009	1-arcsecond
	2	(NASA/METI/AIST/Japan Spacesystems and	2011	1-arcsecond
	3	U.S./Japan ASTER Science Team, 2019)	2019	1-arcsecond
COPERNICUS	1	ESA (Copernicus DEM, 2021)	2019	1-arcsecond
CoastalDEM	1.1	Climate Central	2018	3-arcsecond
	2.1	(Kulp and Strauss, 2018)	2022	3-arcsecond

One solution to circumvent this limitation can be a height correction of SRTM (Figure 2(b)) based on CoastalDEM (Figure 2(a)). To that end, an offset map representing the difference between SRTM and CoastalDEM is created (Figure 2 (c)) and downscaled using a surface spline interpolation. This offset map is then added to the SRTM, which results in a height-corrected, higher-resolution elevation model (Figure 2 (d)). Depending on the use case, the resulting elevation model can be



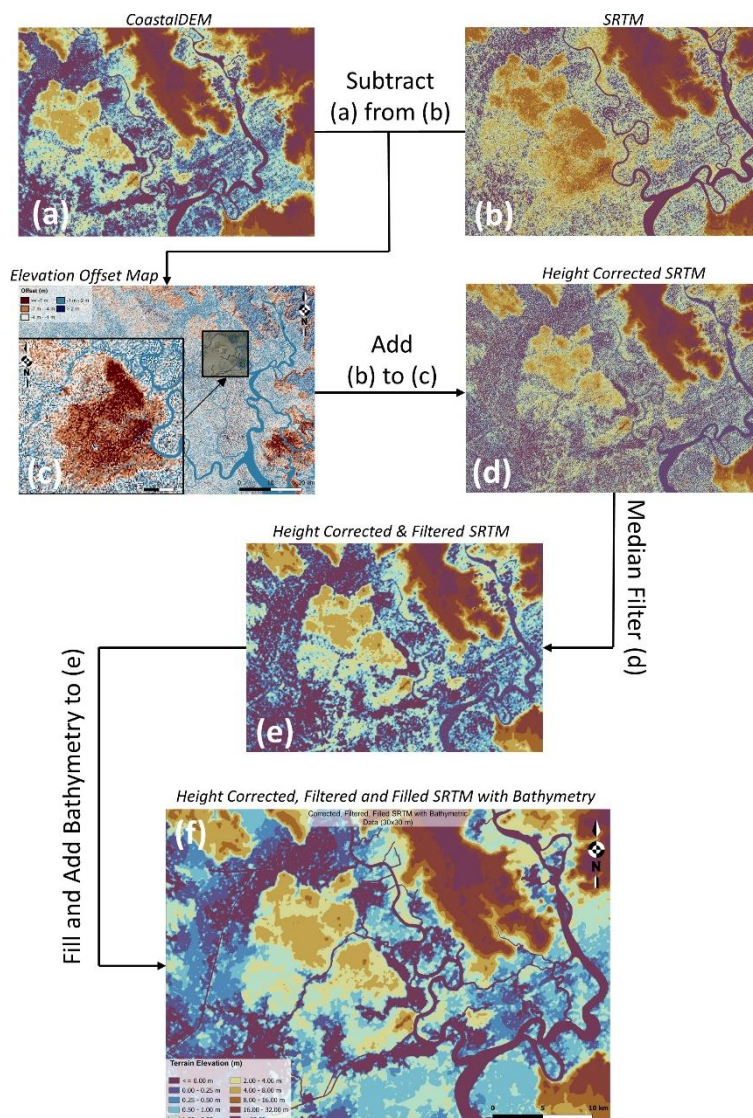
further processed through the use of a 2D median filter (Figure 2 (e)) to smooth out the surface and reduce noise (Ansari and
125 Buddhiraju, 2018). Furthermore, filling algorithms can be used to counteract artifacts causing sinks and holes with no physical
meaning that typically arise in remote sensing. These sinks and holes can be closed by a variety of methods. A comprehensive
list of filling algorithms can be found in the works of Lindsay (2016). It is recommended to first use these after incorporating
bathymetric data (Section 2.1.2) into the DEM (Figure 2 F) to guarantee proper water routing (i.e., from higher lying to lower
lying cells).

130 In the case of HCMC, the adequacy of these five elevation models was assessed by considering their terrain elevation at the
inner-city canal banks that are regular inundation hotspots. Only CoastalDEM delivered a plausible average terrain elevation
of 0 m ASL (Above Sea Level) at this location, while all others returned average terrain elevations of +6 m and higher. As this
level is far above storm surge peak water heights (FIM, 2013), the comparison suggests the best accuracy for CoastalDEM.
An adequate representation of the canal bank elevations is especially important for flood modeling in HCMC, since riparian
135 areas are highly exposed to flooding through storm surges and because such events cause significant backwater effects that
have a crucial impact on water drainage.

To evaluate the accuracy of the end result, a statistical comparison was made between the final DEM and 3 LiDAR data
samples from 2020 in HCMC, whose locations can be found in Figure 3 (Table 2). In all cases, a negative mean error was
calculated, pointing towards an underestimation by the generated DEM. However, a significant deviation can be observed
140 between the calculated errors for each individual sample, whereby the differences to sample A, located on the right Sai Gon
River bank, are roughly twice as large as the differences in samples B and C. These differences will be further discussed in
Section 4.

Table 2. A statistical comparison of the DEM generated through freely available data with 3 LiDAR data samples

Final DEM Comparison with LiDAR Samples					
LiDAR Sample	Area (Km ²)	Absolute Mean Error (m)	Mean Error (m)	Root Mean Square Error (m)	Standard Deviation (m)
A	1.42	1.75	-1.61	2.06	1.29
B	1.42	1.07	-0.87	1.21	0.83
C	1.42	0.86	-0.66	1.04	0.80
Total	4.26	1.24	-1.07	1.52	1.09



145

Figure 2. TERRAIN DATA (A) represents the CoastalDEM, which is subtracted from the SRTM shown in (B) to produce the elevation offset map presented in (C). (D) is the result of adding (B) to (C). (E) depicts the result of the 3x3 2D median filter, which was then filled and enriched with bathymetric data, leading to the final elevation model shown in (F). Topographic data visualized using scientific color maps created by Cramer (2021).

150 **2.1.2 Bathymetric Data**

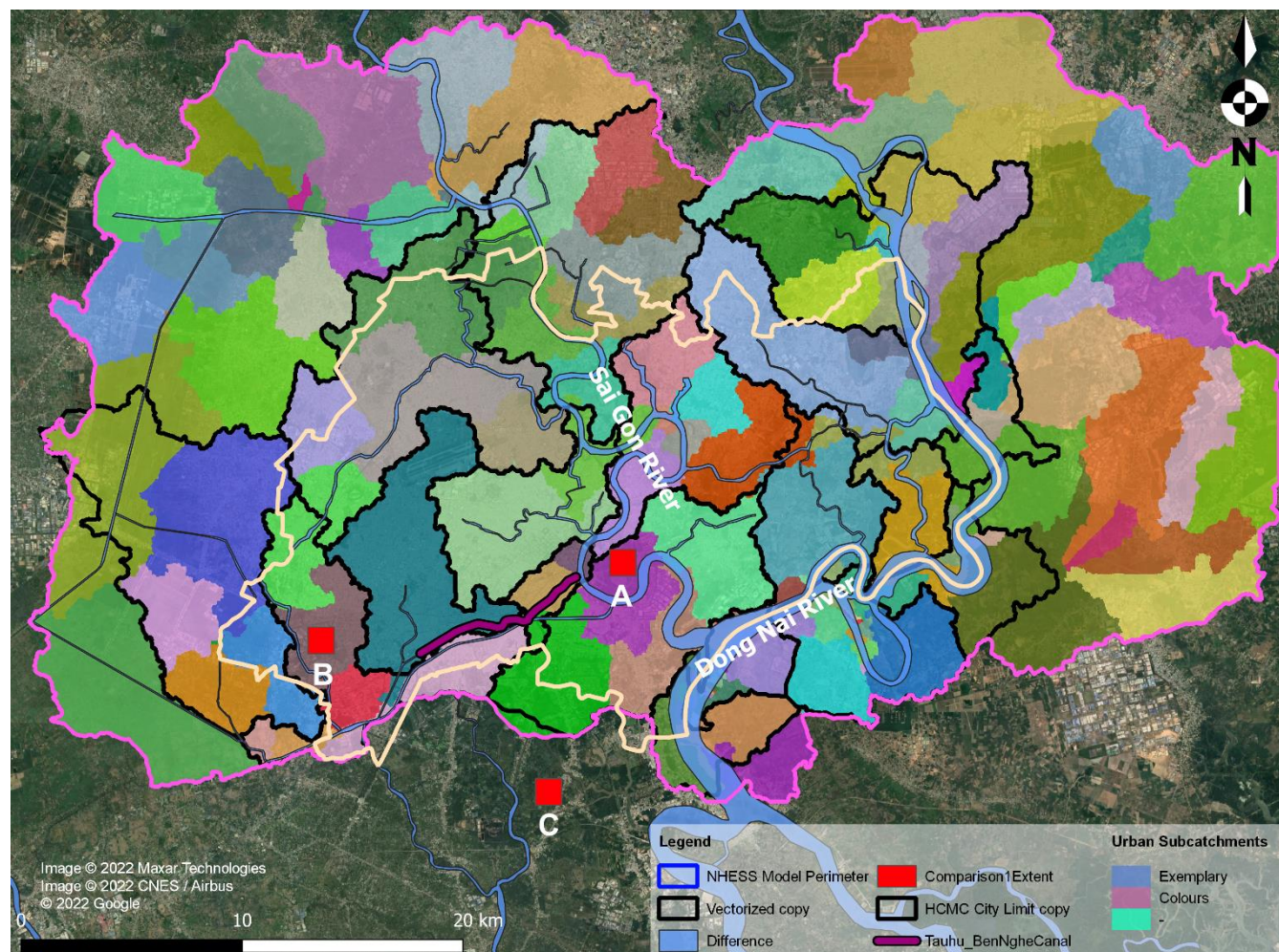
An intrinsic drawback of satellite-based DEMs is the inability of the synthetic aperture sensors (SAR) to determine the geometry of river beds (Farr et al., 2007). Additionally, the generated pixels include surrounding regions, resulting in greatly overestimated main channel depth (Yan et al., 2015b). Therefore, bathymetric data from other sources has to be incorporated into any satellite-based DEM. The availability of dependable open-access bathymetric data, with a resolution sufficient for use

155 in flood modeling, greatly differs between countries and is generally more difficult to acquire. To circumvent this problem,



more extensive research for bathymetric data into peer-reviewed articles as well as engineering reports (*grey* literature) is recommended. Where such literature does not exist, river width and depth can either be approximated (Patro et al., 2009; Neal et al., 2012; Yan et al., 2015a), obtained from calculated global river width and depth databases (Yamazaki et al., 2014; Andreadis et al., 2013), or surveyed in waterways with unknown navigational depths.

160 In the example of HCMC, the hydrological situation (Figure 3) is defined by two major streams, namely the Dong Nai River
which passes the urban districts at the eastern city boundary, and the Sai Gon River which enters the urban area at the central
north and flows into the larger Dong Nai at the central south. These water bodies are fed by a complex network of artificial
canals that drain the inner city. The bathymetry of the Dong Nai River can be approximated from a research article by Gugliotta
et al. (2020), who digitized bathymetric maps that were originally prepared by the US Army Corps of Engineers (USACE) in
165 1965. No literature related to bathymetry exists for the Sai Gon, thus requiring an assumption based on official navigation
depths at different shipping terminals along the river. The Sai Gon bed elevation was approximated through interpolation
between locations with known navigation depths (10.5 m at Ben Nghe Port, 8.5 m at Tan Thuan Port, 6.5 m at Truong Tho
Port) (BENNGHE PORT COMPANY LIMITED, 2014; TRAMECO, 2014; SAIGON PORT JOINT STOCK COMPANY,
2019) and extrapolation beyond the most upstream value with a slope of 0.1 %. This slope represents the average of the Sai
170 Gon at its midsection (IGES, 2007) and was extended until the northern boundary of the model. The results of a sensitivity
analysis to quantify the impact of this assumption on the simulation results is presented in Section 3.2. For the inner-city canals,
a survey conducted by JICA (2001) determined the average depth of these canals to range between -1.82 m and -3.82 m. Given
that neither detailed cross-sections nor profiles were available, all identified canals and channels were set to a depth of -3 m.
For the specific case of HCMC, the aforementioned processing steps lead to the final elevation model: a height corrected, 2D
175 median filtered and filled SRTM topography with a 1 arc second resolution that incorporates bathymetric data for all relevant
water bodies (Figure 2 (f)). Based on this model, various local flow catchments can be defined of which, however, not all
contribute to pluvial flooding in the metropolitan area. Therefore, the perimeter of the HCMC flood model is set to include the
central 18 key urban catchments. This allows to limit simulations to the area of interest and hence to decrease computation
times without affecting simulated flood depths. Figure 3 depicts the various catchments that could be derived from the DEM
180 while also showing the most relevant urban catchments, which most significantly contribute to flooding. Although based on
several case-specific simplifications, this methodology illustrates how free satellite-derived DEMs can readily be combined
with public information on river bathymetries and finally lead to an expedient terrain model for hydro-numerical simulations.



185 **Figure 3. URBAN CATCHMENTS** The hydrologic make-up of HCMC, where all of the local catchments that could be determined through the processed DEM are presented. On this basis 18 key urban catchments were defined, which contribute the greatest part to pluvial flooding within the city. The boundary of the hydro-numerical model equals the perimeter of these catchments in order to decrease computation time without affecting simulated flood depths. The random colors of the urban subcatchments are for illustration purposes only.

2.1.3 Hydraulic Roughness Coefficient

190 Geometrical features that are not represented in the DEM are buildings and extensive vegetation that significantly reduce the available cross-section for water routing. This must be considered in the simulated hydraulic roughness, i.e. in the form of Manning's roughness coefficient, through an additional macro-roughness effect that would be neglected if set to the value of, for example, concrete (Taubenböck et al., 2009; Chen et al., 2012; Vojinovic and Tutulic, 2009). HCMC for instance is a densely built urban city, whose surface is mostly composed of asphalt or concrete with very low roughness. To allow for this effect, a roughness coefficient range of 0.05 to 0.105 for urban environments has been proposed following the
195 recommendations given in the *Journal of Research of the US Geological Survey* (Hejl, 1977), whereby specific values depend



on the ratio of built-up to non-built-up areas. In order to determine the optimal roughness coefficient for the presented model, a calibration was undertaken using inundation depths and locations across HCMC provided by local partners for three severe rain events. The simulated flood depths are then compared to the reported flood depths at the respective locations using the coefficient of determination (R^2), the root mean square error (RMSE), the Nash-Sutcliffe Efficiency (NSE), and the percentage bias (PBIAS) to assess the model quality. Following this approach, the best results are obtained for a roughness value of 0.10, which corresponds to the higher bound of the range proposed for mimicking urban settings in the literature (Schlurmann et al., 2010). The model is validated subsequently for this value using a fourth, independent rain event. Detailed results of this validation are presented in section 3.1.

2.2 Hydro-meteorological Boundary Conditions

As in the case of terrain and bathymetric data, the availability of data pertaining to hydro-meteorological boundary conditions varies widely depending on the region to be modeled. Nevertheless, a similar approach can be adopted as proposed for the elevation data, whereby information and data originating from official sources have the highest priority, followed by open-source repositories, peer-reviewed literature, grey literature, and regional models in descending order of importance. Generally, raw time series allow for independent determination of intensities and return periods of extreme events by fitting the data to a probability function, e.g. Gumbel, Fréchet, or Weibull distributions. A review of this methodological approach can be found in Hansen (2020). However, when there is consensus in the literature, such time series in sufficient temporal resolution, i.e. daily or even monthly cumulative data are absent, or an independent statistical analysis is not necessary, extreme values from literature can be used. This process can be illustrated through the example of HCMC where riverine, tidal, and precipitation boundary conditions are needed. Nonetheless, the focus, in this case, was on heavy rain, which is why the exemplary probabilistic analysis will only be shown for precipitation data.

2.2.1 River Discharge Data

Discharge data is typically readily available, especially in the presence of reservoirs along a river. However, although both the Sai Gon and the Dong Nai Rivers are regulated by upstream reservoirs, no open-access discharge data exists following the FAIR principles in data policy and stewardship (GOFAIR, 2016; Wilkinson et al., 2016; Mons et al., 2017). Nevertheless, singular extreme discharge rates and their respective return periods can be found in the additional material of a research article by Scussolini et al. (2017). Furthermore, long-term mean river discharges of 54 m³/s for the Sai Gon and 890 m³/s for the Dong Nai were reported by Tran Ngoc et al. (2016). Extreme values can be used to investigate fluvial flooding while the average values are of use when investigating the influence of other flood drivers in isolation. Notwithstanding the indisputable temporal variability of river discharge in nature, stationary flow conditions can be assumed for the upstream boundaries of many flood models. Specifically, this holds for all settings, in which other flood drivers with significantly higher rates of change exist, such as in coastal storm-surge or rainfall run-off models (Sandbach et al., 2018). For the case of HCMC, it is assumed that

both the lowland location of the model domain and officially operated reservoirs upstream of the Sai Gon and Dong Nai Rivers justify this simplification.

230 2.2.2 Tidal Data

Although an official gauge station exists at Nha Be (Location in Figure 6), directly at the southern boundary of the HCMC model domain, the corresponding tidal time-series are not publicly available. Nevertheless, data from about 300 tide gauge stations is obtainable from the public repository of the University of Hawaii Sea Level Center including a station in Vung Tau (Caldwell et al., 2015). This gauge is located around 70 km downstream of Nha Be at the South China Sea and documents the
235 period of 1986–2002 and 2007–2021 almost consistently. To extrapolate that time series to the southern boundary of the model, a linear increase in the water levels can be assumed: as Gugliotta et al. (2019) report, high and low water levels steadily increase with a factor of 1.05 between Vung Tau and Nha Be.

In order to validate this approach, official Nha Be tidal time series were compared to the publicly available Vung Tau tidal time series. In fact, after adjusting for a temporal phase shift of 1.8 hours, a linear regression of all data points returns a slope
240 of 1.05. This result corroborates the findings of Gugliotta et al. (2019) in regards to the water level relation between Vung Tau and Nha Be all the while validating the proposed approach. The drawback of such an approach is the inability to calculate the temporal phase shift in water stages and discharges between Vung Tau and Nha Be.

The scaled tidal data can be probabilistically analyzed for the determination of extreme tidal water levels if needed. In the present study case, an eight-day time series representing mean tidal conditions is used as the southern boundary of the hydro-
245 numerical model.

2.2.3 Precipitation Data

In the example of HCMC, precipitation heights related to heavy rain with return periods of 5 years and less vary greatly in existing literature (Minh Nhat et al., 2006; Viet, 2008; FIM, 2013; Loc et al., 2015; Quan et al., 2017; Khiem et al., 2017). In particular, the values for a storm of 3-hour duration and 2-year return period range from 28 mm/hour to 45 mm/hour,
250 warranting an independent statistical analysis. Daily precipitation time series for the Tan Son Hoa weather station in central HCMC spanning from 1960 to 2012 can be obtained from the repository of the National Oceanic and Atmospheric Administration (NOAA), which publishes quality-checked precipitation data for several weather stations across the globe (NOAA, 2022). To determine the daily extreme precipitation depth for the return periods of 2 years and greater, the data is fitted to a Gumbel distribution, where the mean \bar{y}_n and standard deviation σ_n of the Gumbel variate are taken as a function of
255 the record length which is equal to the number of years ($n = 28$):

$$P_{T,24h} = \bar{P} + \left[\frac{-\log(\log(T/(T-1))) - \bar{y}_n}{\sigma_n} \right] \sigma \quad (1)$$



where \bar{y}_n is 0.5343 and σ_n is 1.1047 for $n = 28$ (Selaman et al., 2007). Using the Cramér-von Mises criterion, a $n\omega^2$ of 0.2831 is calculated, which satisfies testing for $\alpha = 0.1$ (Dyck, 1980). In contrast, the probability of occurrence for return periods of 2 years and less can be calculated based on ranking the precipitation depth of the raw data, then using:

$$\frac{2i - 1}{2n} \quad (2)$$

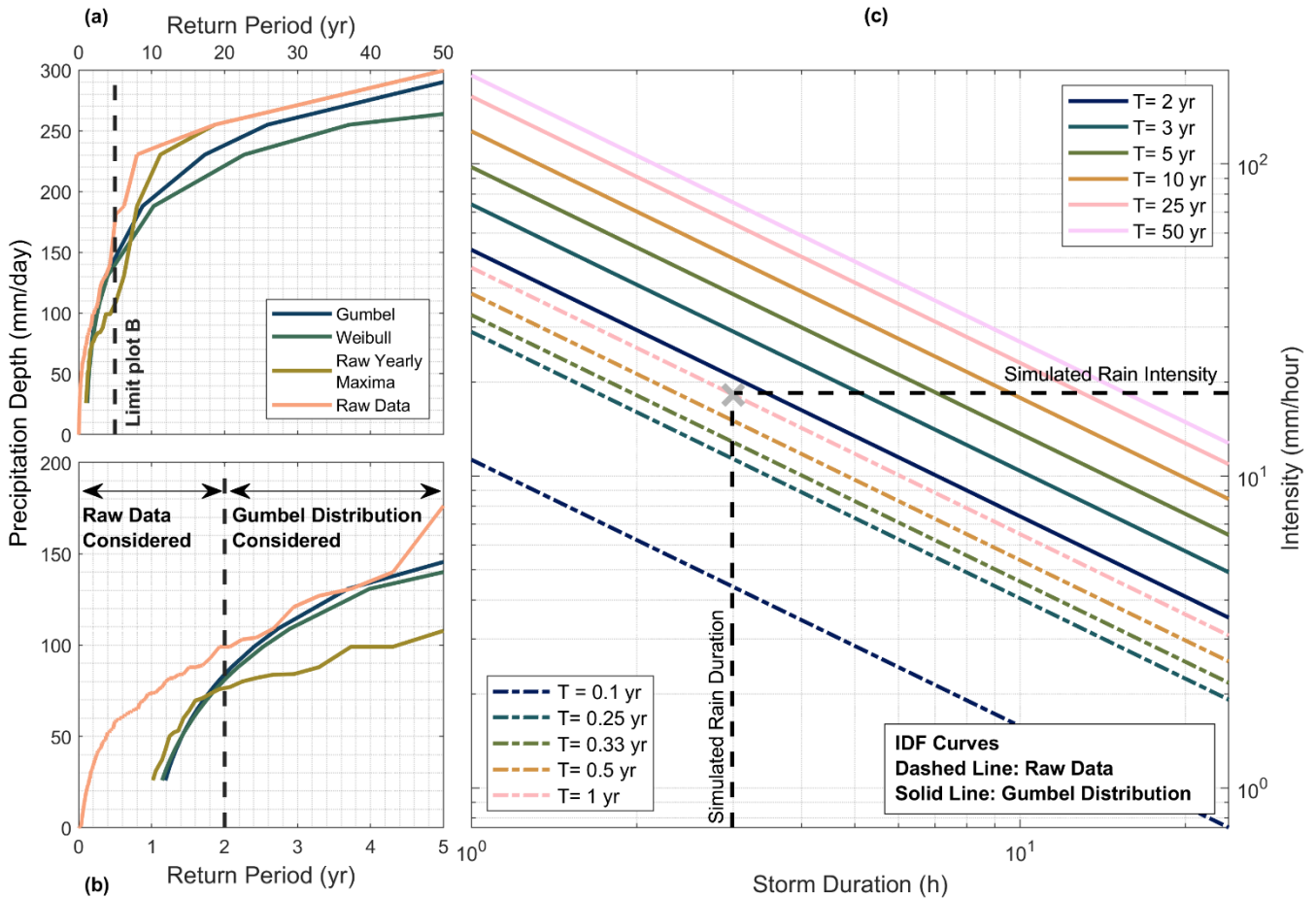
where i the rank of the data point and n is the total number of data points. Given the 24 hours temporal resolution of the raw data, a scaling function is applied to determine the intensities for lower durations (Menabde et al., 1999):

265

$$i_{T,d} = \frac{P_{T,D}}{D} \left(\frac{d}{D} \right)^{-\beta} \quad (3)$$

where $i_{T,d}$ is the intensity for duration d and return period T , $P_{T,D}$ is the precipitation depth to be scaled and β is the scaling factor. Based on the literature average, the latter parameter is assumed to equal 0.854 (Minh Nhat et al., 2006; Khiem et al., 2017). The ensuing Intensity-Duration-Frequency (IDF) curves, which reflect the precipitation depth as a function of storm return period and duration, are presented in Figure 4.

270



275 **Figure 4. INTENSITY-DURATION FREQUENCY** (A) depicts the return period of heavy rain events plotted against the precipitation depths for the raw data, the raw yearly maxima, the Weibull distribution and the Gumbel distribution. (B) zooms in from (A) for the return period of 5 years and less, showing for which return periods the probability of occurrence and the Gumbel distribution are taken into consideration. (C) is the end result, showing the different IDF curves for return periods of 0.1 to 5 years. Data visualized using scientific color maps created by Cramer (2021).

Using official hourly precipitation data for the Tan Son Hoa weather station over the same period, the performance of the NOAA time series as well as the adequacy of the temporal scaling factor β was evaluated (Table 4). The mean value of the
 280 daily yearly maximum precipitation is 94.7 mm and 104.3 mm while the standard deviation is 69.13 mm and 40.64 mm for the NOAA and the official hourly precipitation data respectively. The similarities and differences between the statistical results of both time series will be further discussed in Section 4.

285



Table 3. A statistical comparison of the NOAA and official hourly precipitation data along with a measure of the goodness of fit using the average temporal scaling factor from literature as well as the temporal scaling factor fit to the official data

Validation of the IDF Curves											
Return Period (Years)	Calculated Daily Cumulative Rain (mm)		Best β Value Fit to Official	Goodness of Fit using $\beta = 0.854$ (A) and Best β Fit Value (B)							
	NOAA	Official		SSE		R ²		Adjusted R ²		RMSE	
				A	B	A	B	A	B	A	B
1	73.9	90.5	0.883	373	210	0.838	0.912	0.865	0.924	7.89	5.92
2	84.3	97.6	0.871	219	130	0.913	0.948	0.927	0.957	6.04	4.66
3	117.8	114.6	0.863	18	25	0.994	0.992	0.995	0.994	1.75	2.03
5	155.2	133.5	0.856	280	303	0.930	0.925	0.942	0.937	6.84	7.10
10	202.2	157.3	0.850	1324	1199	0.748	0.772	0.790	0.810	14.85	14.13
25	261.5	187.3	0.844	3779	3107	0.464	0.559	0.553	0.633	25.13	22.76
50	305.5	209.6	0.841	6421	5104	0.250	0.404	0.375	0.503	32.71	29.17

290 As for the creation of an adequate hyetograph, i.e. the development and representation of precipitation depth over time,
 numerous algorithms for the creation of a design storm are available (Balbastre-Soldevila et al. (2019). For rain events in
 HCMC, the linear/exponential synthetic storm of Watt et al. (1986) has been taken to create the hyetograph of a 3-hour
 duration, 1-year return period rain event since it matches the hyetograph according to decision 752/QD TTg of the HCMC
 government. The simple example of deducing the river discharge, tidal water levels, and precipitation hyetograph for HCMC
 295 illustrates, how open data, even if not in the form of time series, can be utilized to define reasonable boundary conditions for
 an urban flood model.

2.3 Processing of Flood Simulation Results

2.3.1 Use of Difference Plots

Ultimately, the presented methodology allows for setting up a hydro-numerical flood model that simulates surface run-off in
 300 an urban setting, in which urban features cannot be fully represented, e.g. exclusion of small-scale topographic elements like
 flood protection structures (artificial bank elevation, flood protection walls and dikes, etc.) or underground systems like
 technical details of a local stormwater drainage system. Given the regional scale of many models, however, it is assumed that
 the absence of the latter is compensated by the hydraulic efficiency of a smoothed and filled DEM, which guarantees that water
 always flows towards the lowest elevations driven by gravity, effectively mirroring the functions of a stormwater drainage
 305 system. In contrast, the absence of flood protection structures in the model has a significant impact on the run-off dynamics in



the model, whereby flooding can even occur in places, where under normal conditions, i.e., no rain, mean tide, mean river flow, no inundation is plausible. To counteract this effect, simulated water levels can be corrected by taking the results of the normal conditions as a reference. Accordingly, only the additional flooding (above regular inundations) is considered as the actual level of flooding, when simulating events with more intense conditions. In order to isolate the impacts of additional flooding, the results of the simulation under normal conditions are then withdrawn from the results of simulations under more intense conditions either occurring in combination or in isolation.

In the HCMC example, the 1-year return period, 3-hour duration (3h1y) rain event is taken for detailed investigation. The reason for this choice is that these yearly recurring events are not usually put into focus when conducting flood simulations, although they bring about major GDP loss that is comparable to and sometimes even greater than major flood events (ADB, 2010). In turn, the results of the simulation under long-term average tidal and riverine conditions are withdrawn from the results of the simulation for the 3h1y rain event with mean tide and mean river discharge. These difference plots finally reflect the extents and dynamics of typical inundations induced by the isolated 3h1y rain event. This methodological approach can be easily applied to a variety of scenarios and corresponding simulations.

2.3.2 Flood Intensity Proxies

Typically, maximum simulated flood depths are used to assess and visualize the *intensity of flooding* in a predefined area. Although this value is a good indicator of the exposure and scale of affected people and tentative damaged areas during extreme events, it lacks elucidating an accurate estimate of projected damages or losses. This is especially important when taking into consideration that, particularly in coastal cities, certain flood depths can persist for a much longer time than others due to tidally induced backwater effects (Andimuthu et al., 2019). This flood duration, on the other hand, is very important when events of marginal intensity, i.e. high probability of occurrence, are investigated since it can be an indicator for the persistence of economic and social disruption (Wagenaar et al., 2016; Koks et al., 2015; Feng et al., 2017; Wagenaar et al., 2017; Thielen et al., 2005; Shrestha et al., 2016; Nizam Ismail, 2020; Debusscher et al., 2020; Molinari et al., 2014) in residential and industrial areas (Tang et al., 1992), as well as in an agricultural context (O'Hara et al., 2019). This effect can best be expressed through the creation of a *duration over threshold* map, which depicts how long a certain flood depth is exceeded. This threshold value can be adjusted according to the local constraints. In the case of HCMC, the threshold depth is set to 0.10 m, given that this value corresponds to the minimum reported flood depth provided by local partners.

In an approach of combining these two perspectives on flood intensity and duration, a simple 2-parametric, but more integrative proxy, defined as the *normalized flood severity index* (NFSI), is proposed in the present paper for the first time in literature. This proxy helps to identify areas, where the combination of both time-independent maximum flood depth and the duration over threshold is at its maximum, and where, accordingly, the largest flood impacts and, thus, most severe damage potential that has been previously hidden can be expected in relation to other areas. The dimensionless NFSI at each grid cell (x,y) can be expressed as follows:



$$NFSI(x, y)(\%) = \frac{z_{max}(x, y) * DoT(x, y)}{\max(z_{max}(x, y)) * \max(DoT(x, y))} * 100 \quad (3)$$

340 where $z_{max}(x, y)$ refers to the maximum simulated flood depth for the depicted scenario being investigated at the local cell
with coordinates x and y in the DEM, and $DoT(x, y)$ refers to the scenario-based simulated inundation duration over a pre-
defined threshold.

3 Model Performance

Even in cases where topographic and hydro-meteorological data is sparse or hard to obtain, it should always be possible to
gather the most essential boundary conditions and compose a basic hydro-numerical model following the aforementioned
methodology. To showcase the applicability and performance of this approach, the following section provides information
regarding the validation results for the exemplary surface runoff model of HCMC as well as a sensitivity analysis that
scrutinizes the validity of the described assumptions concerning the local bathymetry. Subsequently, the simulation results are
analyzed using the indicators and parameters defined in Section 2.6 to determine flooding hotspots. Data on inundation depths
and locations provided by local partners are used in a subsequent step to cross-check the performance of the latter and newly
proposed flood intensity proxy, the NFSI.

3.1 Model Validation

The validation of the model is accomplished by simulating a torrential rain event that occurred during the monsoon season on
06/14/2010. During this event, a total of 73 mm of rain fell on HCMC, flooding a total of 25 observation points scattered
across the city. The maximum flood inundation depths were determined using the difference plot method depicted in
section 2.3. These are then compared with the reported flood depths at the 25 observation points depicted in Figure 5 using R^2 ,
NSE, RMSE, and PBIAS. The values strongly suggest the validity of the employed methodology.

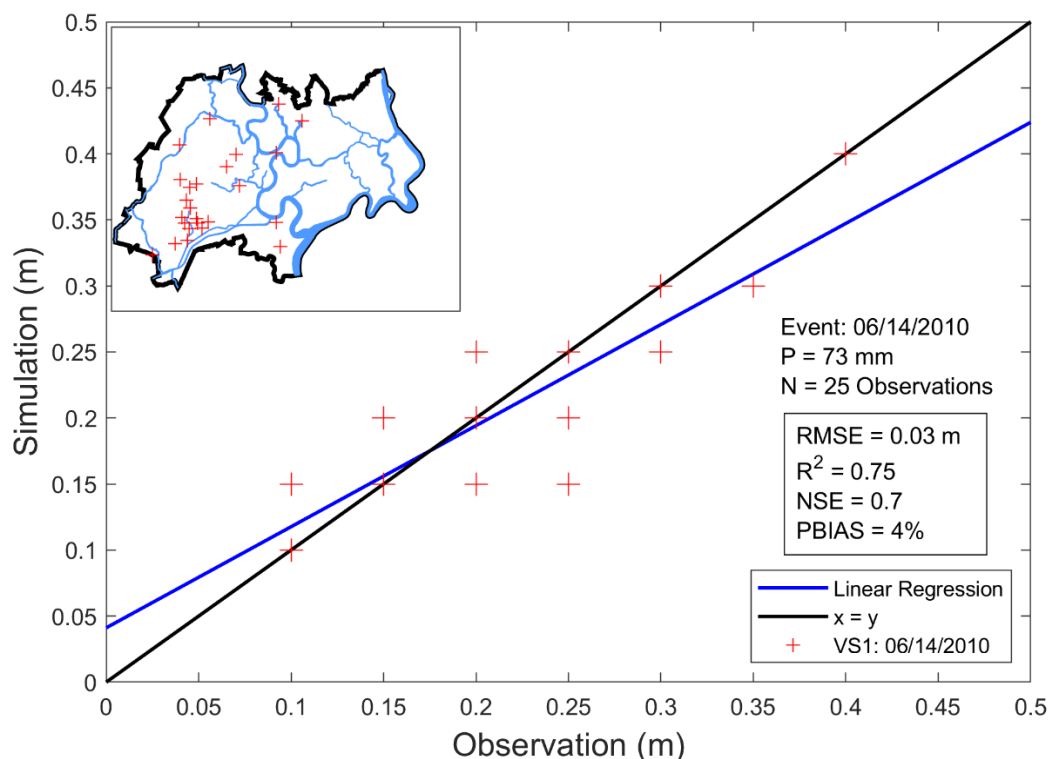
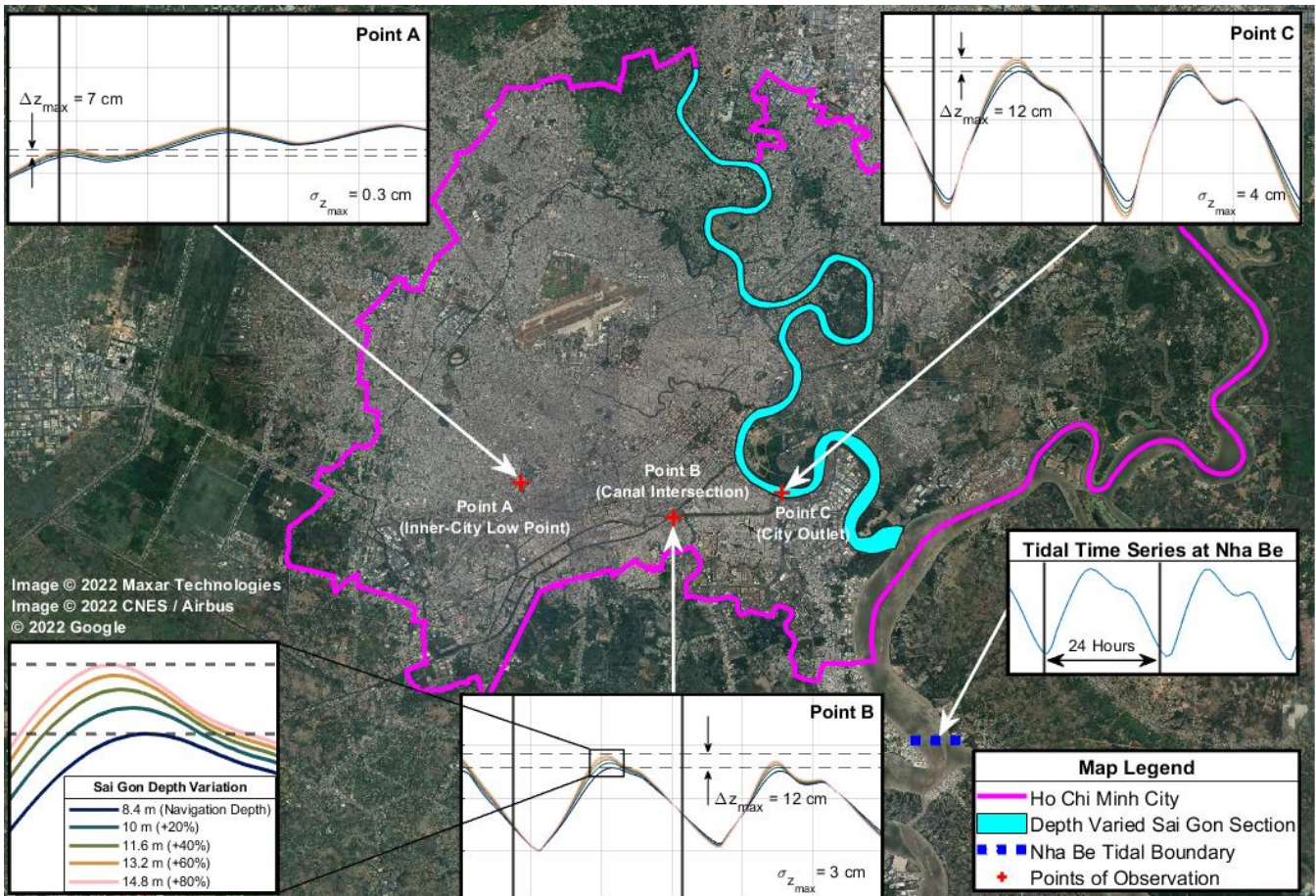


Figure 5. MODEL VALIDATION: Simulated flood depths are plotted against the reported flood depths at the 25 points of observation (red crosses) along with the linear regression (in blue) and the calculated R^2 , NSE, RMSE and PBIAS (bottom right).

360 3.2 Sensitivity Analysis for the Assumed River Bed Elevation

Given that the Sai Gon bathymetry is approximated by assumptions that are solely based on the officially maintained fairway depth, it seems reasonable to assess the sensitivity of simulation results to variations of water depth in the Sai Gon River. The river bed elevation is thus varied between 1.0 and 1.8-fold of the navigation depth in increments of 0.2. The results of this simulation are shown in Figure 6. Specifically, the simulated water surface levels increase at points A (inner-city low point),
365 B (canal intersection), and C (city outlet) with increasing river bed elevation. Nevertheless, the maximum nominal difference in the water surface levels is 7 cm at point A, and 12 cm at both B and C. Comparing depths of 1.2 times and 1.8 times the fairway depth, this difference is 4 cm at point A, which can be considered negligible. Given the low sensitivity of the water surface level to the depth of the Sai Gon, employing the assumption stipulated in section 2.1.1 is rendered sufficient for the flood model.



370

Figure 6. DEPTH SENSITIVITY: Impact of varying the depth of Sai Gon River on water depth at three different locations (Inner-City low point, canal intersection and city outlet). Data visualized using scientific color maps created by Crameri (2021).

3.3 Performance of the Flood Intensity Proxies

The 3-hour duration, 1-year return period rain event with a precipitation depth of 54 mm can be investigated using the flood intensity proxies defined in Section 2.3.2. Comparing Figures 6(a) and 6(b) shows a relationship between maximum flood depth (mFD) and duration over threshold (DoT). However, a high mFD does not necessarily translate to a high DoT and vice versa as evident by the areas on the western bank of the Sai Gon River. At this location, a relatively high mFD but a relatively short DoT can be observed. This example epitomizes the usual shortcomings of using only one of the classical proxies for assessing flood damage potential. Combining these into a 2-parametric NFSI that was normalized for the *max* results in a map that highlights previously hidden inundation hotspots with significant damage potential due to flooding (Figure 7 (c)). The locations of reported inundations and the NFSI heat map show considerable spatial overlapping, whereby around 73% of the reported inundations lie inside or within 100 meters of the areas highlighted by the NFSI which only cover 19% of the total area of HCMC, as opposed to 78% and 73% for the mFD and DoT, that 38% and 34% of the area respectively (Table 4). The

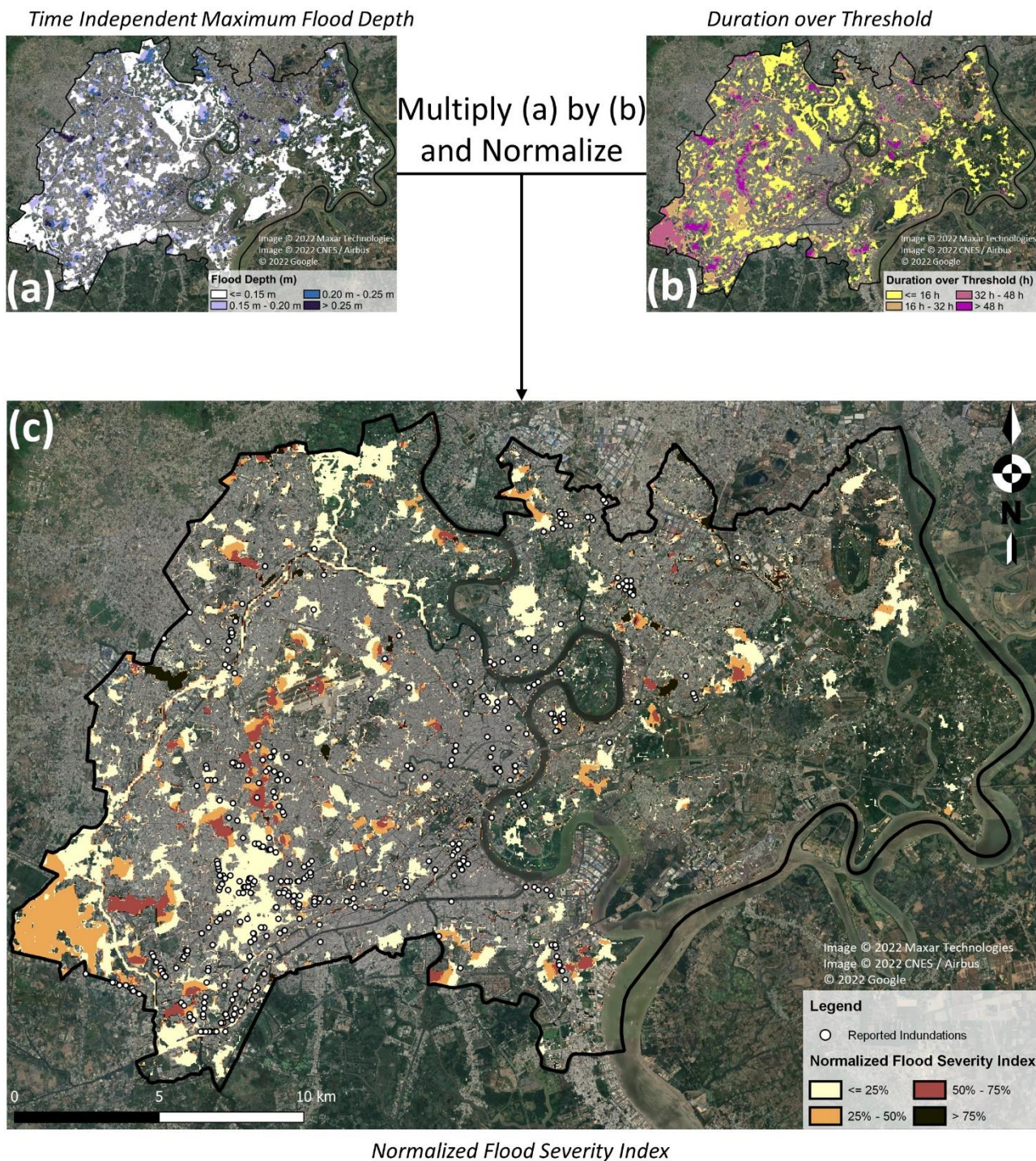
380



385 small spatial extent of the NFSI heat map, relative to the mFD and DoT maps, coupled with the relatively high coverage of reported flooding locations corroborates the usefulness of the proposed index in successfully identifying the spatial extents of flooding hotspots.

Table 4. Performance of the different flood proxies in terms of the spatial overlapping with the locations of reported inundations

Flood Proxy	Spatial Overlap with Reported Inundations (%)	Area Coverage (%)	Accuracy Ratio vis-à-vis a Random Area with Equal Coverage
Maximum Flood Depth	78%	38%	2.05
Duration over Threshold	73%	34%	2.15
Normalized Flood Severity Index	73%	19%	3.84



390 **Figure 7. FLOOD INTENSITY (A)** depicts the time-independent maximum flood depth in meters, while **(B)** depicts the duration over a threshold of 10 cm in hours. **(C)** reveals the results of the normalized flood severity index (NFSI), whereby hotspots of this index (covering 19% of HCMC) show a high spatial overlapping with the reported inundations (73% inside or within 100 m). Data visualized using scientific color maps created by Crameri (2021).



4 Discussion

395 Since topographic data plays a significant role in flood modeling, its validation is imperative. However, difficulties in this
 respect arise from the lack of ground truthing data in many countries, if local topographic surveys or LiDAR data are
 inaccessible. The only data close to ground truth in the case of HCMC is the JICA report from 2001 (JICA, 2001), in which
 various canal bank elevations can be found. Furthermore, there is a substantial difference between high-resolution LiDAR data
 and satellite-derived DEMs that cannot be closed independent of the amount of processing. As for the satellite DEMs, there
 400 exists a multitude of such models that need to be carefully considered for each specific task. Some more recently provided
 terrain and elevation models, like the CopernicusDEM, do offer advantages in terms of lower noise levels and resolution, but
 do not represent the elevation of the actual surface in an urban environment which is especially problematic in urban coastal
 agglomerations, where flawed terrain elevation can have a significant impact on flooding extent due to tidal effects. Even the
 assumption that CoastalDEM represents the actual surface elevation is vague in the context of Southeast Asian coastal cities.
 405 In fact, Vernimmen et al. (2020) calculated an average error for the Mekong Delta area in Vietnam of +1.23 m for the SRTM
 and -1.35 m for the CoastalDEM, concluding that the SRTM generally overestimates surface elevation, while CoastalDEM
 underestimates it. Building on that approach, a comparison of the performance of the various DEMs in terms of representing
 the canal bank elevations reported by JICA (2001) can be undertaken for the Tau Hu - Ben Nghe Canal (Figure 3), with the
 results shown in Table 5.

410 **Table 5. Comparison of accuracy for the various freely available satellite-based DEMs with ground truth data found in the JICA
 report for the Tau Hu - Ben Nghe canal bank elevations, showing an overestimation for the SRTM, ALOS, ASTER, CopernicusDEM
 and CoastalDEM v 2.1, and an underestimation for the CoastalDEM (JICA, 2001).**

Tau Hu - Ben Nghe Canal Bank Elevations							
	JICA	SRTM	ALOS	ASTER	CopernicusDEM	CoastalDEM v 1.1	CoastalDEM v 2.1
Minimum (m ASL)	+0.9	+7.4	+6.6	+7.6	+4.3	-2.1	+2.3
Maximum (m ASL)	+2.9	+13.2	+40.1	+17.7	+12.1	+1.0	+8.2
Average (m ASL)	+1.8	+5.9	+9.1	+11.3	16.2	-0.3	+3.2

Table 5 reveals similar findings to those of Vernimmen et al. (2020), whereby the Tau Hu - Ben Nghe canal bank elevation is
 415 overestimated by +4.1 m on average in the SRTM while being underestimated by -2.1 m in the first version of CoastalDEM,
 thus corroborating the conclusions reached by Schumann and Bates (2018) on the inadequacy of most open access DEMs in
 flood simulation, especially in urban environments. The newer version of the CoastalDEM (CoastalDEM v 2.0), with
 supposedly improved accuracy, overestimates the canal bank elevations and shows a great divergence from CoastalDEM v 1.1,
 which highlights the difficulty of accurately representing topography in dense environments even with the help of artificial
 420 intelligence.

These findings were further reinforced by the comparison results of three LiDAR data samples provided by local partners and
 the end product DEM presented in Section 2.1.1, whereby a negative mean error could be observed, pointing to an
 underestimation of terrain elevation. However, this error (-1.61 m) was greatest in the LiDAR sample A, where the biggest



differences were observed at the location of high-rise buildings, followed by sample B (-0.87 m), where again the biggest
425 differences were observed at the location of buildings. At the relatively unbuilt sample C, the mean error was -0.66 m, which
might point towards the existence of a certain offset between the final DEM and the LiDAR data. However, given the small
sample size (4.26 Km²), it is difficult to make a definitive conclusion on the validity of the final DEM solely based on this
comparison. But combined with the other observations, it can be said that the SRTM correction based on CoastalDEM tends
to underestimate terrain elevation. Nevertheless, the final DEM exhibits errors that are far less than those found in the other
430 open access DEMs relative to the Ben Nghe canal bank elevations. Additionally, the topography of HCMC is affected by
varying degrees of land subsidence, ranging from 0.33 cm to 5.3 cm/year (Duffy et al., 2020) and even reaching 8 cm/year in
some areas (Ho Tong Minh et al., 2020), exacerbating the uncertainty in elevation. Nevertheless, in the presented workflow,
the underestimation of the CoastalDEM is successfully counteracted with the use of difference plots (cf. details in Section
2.3.1), through which only additional water levels (in excess of the normal conditions) are considered as actual flooding.
435 Backed up by the model calibration and validation, the joint use of the end result of the DEM processing and the difference
plots delivers flood simulation results that successfully reproduce known inundation hotspots in HCMC.

In terms of the roughness coefficient, the optimal value determined through model calibration matches the value of a more
recent study by Beretta et al. (2018), who concluded that using a roughness coefficient of 0.10 in the absence of buildings had
similar flood results to incorporating those elements. This reinforces the idea that replacing buildings with a higher (macro-)
440 roughness coefficient could account for the obstruction effect seen during urban floods when only coarse elevation data is
available. However, another method that was implemented by Taubenböck et al. (2009) and Schlurmann et al. (2010) lies in
the usage of a building mask within the DEM as a replacement to mimic infrastructure footprint and limit flood flow dynamics
to residual open spaces. Although this method may prove useful in case the resolution of the DEM is 10 m or higher, it might
not be easily implemented at DEM resolutions of 30 m or coarser given in the present case. In this regard, the elevated
445 roughness coefficient offers an adequate solution that does not substantially alter the maximum flood depths and durations,
especially when considering that building themselves are not impermeable, whereby basements can easily get flooded during
rain events (Sandink, 2016).

Looking at the tidal data, the proposed methodology has a shortcoming regarding the temporal phase shift between the tidal
time series at Vung Tau and Nha Be. However, it can be assumed that this relatively small phase shift (1.8 hours) has a
450 negligible impact when investigating flooding or backwater effects during storm events given that the phase shift between the
start of a rain event and high water is of more importance than the phase shift between Vung Tau and Nha Be.

Comparing the open-access daily precipitation time series with the official hourly precipitation time series at the Tan Son Hoa
weather station shows a certain discrepancy between the two data sets which becomes evident when comparing the mean
values (94.7 mm vs 104.3 mm) and standard deviation (69.13 mm vs 40.64 mm) of the daily yearly maxima. The effect of this
455 discrepancy, driven mainly by the big difference in the standard deviation, can especially be seen for the higher return period
intensities. As for the temporal scaling factor β , the fitting to the hourly precipitation data reveals that β decreases with
increasing return periods, where the average value of 0.858 corroborates the average calculated through literature. Taking into



account the variation in β relative to the return period improved the goodness of fit of the temporal scaling function. However, it wasn't enough to offset the discrepancy between the two data series.

460 In regards to the validation and calibration data, it is a well-known problem that reliable measurements of flood depth and extent during urban floods are hard to acquire (Wang et al., 2018). This paper fortunately makes use of reported inundation depths and locations across HCMC that were provided by local partners. To remedy this limitation, it could be argued that existing surveillance cameras throughout cities could be used to monitor time-varying water levels during flooding (Muhadi et al., 2021), which can either be done manually (Liu et al., 2015) or automatically (Moy de Vitry et al., 2019; Feng et al., 465 2020), providing crucial validation data that could go a long way in helping urban flood models become more accurate without additional costs. Furthermore, user-generated images can also offer an additional way of quantifying flooding (Ahmad et al., 2018), whose acquisition became much easier with the proliferation of social media (Chaudhary et al., 2020).

Open-access data do not usually offer the detail required to build flood damage models, which typically require extensive data, whose acquisition is oftentimes laborious and prohibitively costly. The NFSI, presented in Section 2.3.2, combines flood depth and duration, both of which are results of a hydro-numerical model that are used as input in flood damage models. The 470 comparison with known inundation hotspots, as provided by local partners, proved the usefulness of this indicator in estimating concentrated flood risk. One limitation of the NFSI can be seen in the exclusion of flow velocity, which might play a secondary role in flood impact (Wagenaar et al., 2017; Amadio et al., 2019). However, this impact is rather small when compared to those of flood depth and duration, particularly for estimating monetary loss (Kreibich et al., 2009), and even more so in the 475 rainfall-runoff scheme. It can also be argued that the NFSI lacks the detail as well as the complexity of sophisticated flood damage models that are based on much more extensive and comprehensive data. However, the purpose of the NFSI concept and demonstrated application is not to replace established flood damage estimations but rather to complement these by enhancing the basic interpretation of hydro-numerical results through the combination of flood depths and durations. This allows it to be an effective tool in terms of a first estimation when striving to determine inundation hotspots by robust 480 mathematical models with high damage potential that demand attention in terms of emergency efforts and/or relief. This tool enables stakeholders as well as researchers to narrow down the scope to the areas with the highest damage potential in order to advance adaptation schemes under climate change and projected impacts in low-elevated coastal zones (Scheiber et al., In Review).

5 Conclusion

485 Hydro-numerical models are a powerful instrument that helps understand the dynamics of urban flooding, assess areas of exposure (hotspots) and progress possible mitigation strategies. In many settings, however, essential information about topographic, bathymetric, and hydro-meteorological constraints is hard to acquire without financial costs, rendering independent but trustworthy analyses and evaluation for adaptation measures difficult. The present paper addresses this shortcoming and presents a methodology to create a surface runoff model for the exemplary case of HCMC solely based on



490 open data sources and according to the FAIR principles (GOFAIR, 2016). The process used to build this schematic yet flexible
model can, at least partially, be used to simulate flood drivers in any urban setting. In addition, a newly proposed flood intensity
proxy with a 2-parametric representation of flood depth and duration, the normalized flood severity index (NFSI), is defined
as a means of locating potential flood damage hotspots. The NFSI successfully uncovered flooding hotspots in HCMC,
whereby 73% of over 300 reported inundations were inside or within 100 m of the NFSI's spatial extent that covered only
495 19% of the total area of the city. The employed methodology and findings add to the current research in urban hydrological
modelling and flood risk management and exemplify, which opportunities lie in the continuously growing amount of freely
available data. At last, it hopefully encourages researchers to make their work accessible and thus contribute to independent
and more equal sciences.

500 **Code availability**

No code was used in this research. Details about the general processing of numerical data are provided in the methods section
or can be inquired from the corresponding author.

505 **Data availability**

The references and freely available data used in this study can be accessed through the respective journals or databases.

Author contributions

510

MHJ, LS and CJ developed the methodology for acquiring, processing and comparing the open-access data, which was then
executed by MHJ. MHJ, LS and JV designed the hydro-numerical model finally set up and operated by MHJ. HQN provided
the hydro-meteorological data required for validation. MHJ and LS developed the Normalized Flood Severity Index. MHJ and
LS developed the underlying paper concept. MHJ wrote the initial manuscript with input from LS, while CJ, JV, HQN and TS
515 edited and contributed to the final text. MHJ and LS contributed to the visualization of the results. JV and TS (co-)designed
the overarching research project, were responsible for funding resources and provided guidance throughout the entire study.

Acknowledgements

The authors wish to express their gratitude towards Dr. Nguyen Quy from EPT Environment & Target Public Ltd for providing
520 us with the locations and depths of reported inundations across a variety of flood events in Ho Chi Minh City that were
necessary for the model validation. Moreover, sincere thanks go to both the editor at NHSS for handling the manuscript and
two anonymous reviewers for their helpful comments.



References

- ADB: Ho Chi Minh City - Adaptation to Climate Change: Summary Report, Asian Development Bank, Manila, the Philippines, 2010.
- 525 Ahmad, K., Sohail, A., Conci, N., and Natale, F. de: A Comparative Study of Global and Deep Features for the Analysis of User-Generated Natural Disaster Related Images, in: 2018 IEEE 13th Image, Video, and Multidimensional Signal Processing Workshop (IVMSP), Aristi Village, Zagorochoria, Greece, 6/10/2018 - 6/12/2018, 1–5, 2018.
- Amadio, M., Scorzini, A. R., Carisi, F., Essenfelder, A. H., Domeneghetti, A., Mysiak, J., and Castellarin, A.: Testing empirical and synthetic flood damage models: the case of Italy, *Nat. Hazards Earth Syst. Sci.*, 19, 661–678, <https://doi.org/10.5194/nhess-19-661-2019>, 2019.
- 530 Andimuthu, R., Kandasamy, P., Mudgal, B. V., Jeganathan, A., Balu, A., and Sankar, G.: Performance of urban storm drainage network under changing climate scenarios: Flood mitigation in Indian coastal city, *Scientific reports*, 9, 7783, <https://doi.org/10.1038/s41598-019-43859-3>, 2019.
- 535 Andreadis, K. M., Schumann, G. J.-P., and Pavelsky, T.: A simple global river bankfull width and depth database, *Water Resour. Res.*, 49, 7164–7168, <https://doi.org/10.1002/wrcr.20440>, 2013.
- Ansari, R. A. and Buddhiraju, K. M.: Noise Filtering in High-Resolution Satellite Images Using Composite Multiresolution Transforms, *PFG*, 86, 249–261, <https://doi.org/10.1007/s41064-019-00061-4>, 2018.
- Balbastre-Soldevila, García-Bartual, and Andrés-Doménech: A Comparison of Design Storms for Urban Drainage System Applications, *Water*, 11, 757, <https://doi.org/10.3390/w11040757>, 2019.
- 540 Barragán, J. M. and Andrés, M. de: Analysis and trends of the world's coastal cities and agglomerations, *Ocean & Coastal Management*, 114, 11–20, <https://doi.org/10.1016/j.ocecoaman.2015.06.004>, 2015.
- Becek, K.: Assessing Global Digital Elevation Models Using the Runway Method: The Advanced Spaceborne Thermal Emission and Reflection Radiometer Versus the Shuttle Radar Topography Mission Case, *IEEE Trans. Geosci. Remote Sensing*, 52, 4823–4831, <https://doi.org/10.1109/TGRS.2013.2285187>, 2014.
- 545 BENNGHE PORT COMPANY LIMITED: Overview, Geographic Location, BEN NGHE PORT, benngheport.com/about-us/overview.html, last access: 22 July 2022, 2014.
- Beretta, R., Ravazzani, G., Maiorano, C., and Mancini, M.: Simulating the Influence of Buildings on Flood Inundation in Urban Areas, *Geosciences*, 8, 77, <https://doi.org/10.3390/geosciences8020077>, 2018.
- 550 Beven, K. J.: *Rainfall-Runoff Modelling: The Primer*, John Wiley & Sons, 2011.
- Bright et al.: *Landscan 2010*, <https://landscan.ornl.gov>, 2011.
- Brown, S., Nicholls, R. J., Lowe, J. A., and Hinkel, J.: Spatial variations of sea-level rise and impacts: An application of DIVA, *Climatic Change*, 134, 403–416, <https://doi.org/10.1007/s10584-013-0925-y>, 2016.



- C.R. Thorne, E.C. Lawson, C. Ozawa, S.L. Hamlin, and L.A. Smith: Overcoming uncertainty and barriers to adoption of
555 Blue-Green Infrastructure for urban flood risk management, *Journal of Flood Risk Management*, 11, S960-S972,
<https://doi.org/10.1111/jfr3.12218>, 2015.
- Caldwell et al.: Sea level measured by tide gauges from global oceans - the Joint Archive for Sea Level holdings (NCEI
Accession 0019568), Version 5.5, NOAA National Centers for Environmental Information, 2015.
- Chaudhary, P., D'Aronco, S., Leitão, J. P., Schindler, K., and Wegner, J. D.: Water level prediction from social media
560 images with a multi-task ranking approach, *ISPRS Journal of Photogrammetry and Remote Sensing*, 167, 252–262,
<https://doi.org/10.1016/j.isprsjprs.2020.07.003>, 2020.
- Chen, A. S., Evans, B., Djordjević, S., and Savić, D. A.: A coarse-grid approach to representing building blockage effects in
2D urban flood modelling, *Journal of Hydrology*, 426-427, 1–16, <https://doi.org/10.1016/j.jhydrol.2012.01.007>, 2012.
- Chu, T. and Lindenschmidt, K.-E.: Comparison and Validation of Digital Elevation Models Derived from InSAR for a Flat
565 Inland Delta in the High Latitudes of Northern Canada, *Canadian Journal of Remote Sensing*, 43, 109–123,
<https://doi.org/10.1080/07038992.2017.1286936>, 2017.
- Copernicus DEM, 2021.
- Cramer, F.: Scientific colour maps, Zenodo, 2021.
- Debusscher, B., Landuyt, L., and van Coillie, F.: A Visualization Tool for Flood Dynamics Monitoring Using a Graph-Based
570 Approach, *Remote Sensing*, 12, 2118, <https://doi.org/10.3390/rs12132118>, 2020.
- Di Baldassarre, G. and Uhlenbrook, S.: Is the current flood of data enough? A treatise on research needs for the improvement
of flood modelling, *Hydrol. Process.*, 26, 153–158, <https://doi.org/10.1002/hyp.8226>, 2012.
- Doocy, S., Daniels, A., Murray, S., and Kirsch, T. D.: The human impact of floods: a historical review of events 1980-2009
and systematic literature review, *PLoS Curr*, 5,
575 <https://doi.org/10.1371/currents.dis.f4deb457904936b07c09daa98ee8171a>, 2013.
- Duffy, C. E., Braun, A., and Hochschild, V.: Surface Subsidence in Urbanized Coastal Areas: PSI Methods Based on
Sentinel-1 for Ho Chi Minh City, *Remote Sensing*, 12, 4130, <https://doi.org/10.3390/rs12244130>, 2020.
- Earth Resources Observation and Science (EROS) Center: Collection-1 Landsat 8 OLI (Operational Land Imager) and TIRS
(Thermal Infrared Sensor) Data Products, 2018.
- 580 Ekeu-wei, I. T. and Blackburn, G. A.: Catchment-Scale Flood Modelling in Data-Sparse Regions Using Open-Access
Geospatial Technology, *IJGI*, 9, 512, <https://doi.org/10.3390/ijgi9090512>, 2020.
- Farr, T. G., Rosen, P. A., Caro, E., Crippen, R., Duren, R., Hensley, S., Kobrick, M., Paller, M., Rodriguez, E., Roth, L.,
Seal, D., Shaffer, S., Shimada, J., Umland, J., Werner, M., Oskin, M., Burbank, D., and Alsdorf, D.: The Shuttle Radar
Topography Mission, *Rev. Geophys.*, 45, <https://doi.org/10.1029/2005RG000183>, 2007.
- 585 Feng, Y., Brubaker, K. L., and McCuen, R. H.: New View of Flood Frequency Incorporating Duration, *J. Hydrol. Eng.*, 22,
4017051, [https://doi.org/10.1061/\(ASCE\)HE.1943-5584.0001573](https://doi.org/10.1061/(ASCE)HE.1943-5584.0001573), 2017.



- Feng, Y., Brenner, C., and Sester, M.: Flood severity mapping from Volunteered Geographic Information by interpreting water level from images containing people: A case study of Hurricane Harvey, *ISPRS Journal of Photogrammetry and Remote Sensing*, 169, 301–319, <https://doi.org/10.1016/j.isprsjprs.2020.09.011>, 2020.
- 590 FIM: Ho Chi Minh City Flood and Inundation Management, Final report, volume 2: IFRM strategy annex 1: Analysis of flood and inundation hazards, Ho Chi Minh City, Vietnam, 2013.
- Gallien, T. W., Schubert, J. E., and Sanders, B. F.: Predicting tidal flooding of urbanized embayments: A modeling framework and data requirements, *Coastal Engineering*, 58, 567–577, <https://doi.org/10.1016/j.coastaleng.2011.01.011>, 2011.
- 595 GOFAIR: Fair Principles, <https://www.go-fair.org/fair-principles/>, last access: 15 September 2022, 2016.
- Gugliotta, M., Saito, Y., Ta, T. K. O., van Nguyen, L., Uehara, K., Tamura, T., Nakashima, R., and Lieu, K. P.: Sediment distribution along the fluvial to marine transition zone of the Dong Nai River System, southern Vietnam, *Marine Geology*, 429, 106314, <https://doi.org/10.1016/j.margeo.2020.106314>, 2020.
- Hallegatte, S., Green, C., Nicholls, R. J., and Corfee-Morlot, J.: Future flood losses in major coastal cities, *Nature Clim Change*, 3, 802–806, <https://doi.org/10.1038/nclimate1979>, 2013.
- 600 Hamel, P. and Tan, L.: Blue-Green Infrastructure for Flood and Water Quality Management in Southeast Asia: Evidence and Knowledge Gaps, *Environmental Management*, 1–20, <https://doi.org/10.1007/s00267-021-01467-w>, available at: <https://link.springer.com/article/10.1007/s00267-021-01467-w>, 2021.
- Hansen, A.: The Three Extreme Value Distributions: An Introductory Review, *Front. Phys.*, 8, <https://doi.org/10.3389/fphy.2020.604053>, 2020.
- 605 Hanson, S., Nicholls, R., Ranger, N., Hallegatte, S., Corfee-Morlot, J., Herweijer, C., and Chateau, J.: A global ranking of port cities with high exposure to climate extremes, *Climatic Change*, 104, 89–111, <https://doi.org/10.1007/s10584-010-9977-4>, available at: <https://link.springer.com/article/10.1007/s10584-010-9977-4>, 2011.
- Hawker, L., Bates, P., Neal, J., and Rougier, J.: Perspectives on Digital Elevation Model (DEM) Simulation for Flood Modeling in the Absence of a High-Accuracy Open Access Global DEM, *Front. Earth Sci.*, 6, <https://doi.org/10.3389/feart.2018.00233>, 2018.
- 610 Hejl, L.: A Method for adjusting values of Manning's Roughness Coefficient for flooded urban areas, *Jour. Research U.S. Geol. Survey*, 5, 541–545, 1977.
- Ho Tong Minh, D., NGO, Y.-N., Lê, T. T., Le, T. C., Bui, H. S., Vuong, Q. V., and Le Toan, T.: Quantifying Horizontal and Vertical Movements in Ho Chi Minh City by Sentinel-1 Radar Interferometry, 2020.
- 615 Hong, H., Tsangaratos, P., Ilija, I., Liu, J., Zhu, A.-X., and Chen, W.: Application of fuzzy weight of evidence and data mining techniques in construction of flood susceptibility map of Poyang County, China, *The Science of the total environment*, 625, 575–588, <https://doi.org/10.1016/j.scitotenv.2017.12.256>, 2018.
- Hu, Z., Peng, J., Hou, Y., and Shan, J.: Evaluation of Recently Released Open Global Digital Elevation Models of Hubei, China, *Remote Sensing*, 9, 262, <https://doi.org/10.3390/rs9030262>, 2017.
- 620



- Huong, H. T. L. and Pathirana, A.: Urbanization and climate change impacts on future urban flooding in Can Tho city, Vietnam, *Hydrol. Earth Syst. Sci.*, 17, 379–394, <https://doi.org/10.5194/hess-17-379-2013>, 2013.
- IGES: Sustainable Groundwater Management in Asian Cities, 2007.
- Intermap: NextMap World 10, <https://www.intermap.com/data/nextmap>, 2018.
- 625 IPCC: Climate Change 2022: Impacts, Adaptation, and Vulnerability, Contribution of Working Group II to the Sixth Assessment Report of the Intergovernmental Panel on Climate Change, Cambridge University Press, 2022.
- Jarhani, A. A., Callow, J. N., McVicar, T. R., van Niel, T. G., and Larsen, J. R.: Satellite-derived Digital Elevation Model (DEM) selection, preparation and correction for hydrodynamic modelling in large, low-gradient and data-sparse catchments, *Journal of Hydrology*, 524, 489–506, <https://doi.org/10.1016/j.jhydrol.2015.02.049>, 2015.
- 630 JICA: Detailed Design Study on HCMC Water Environment Improvement Project (Final Report), Ho Chi Minh City, 2001.
- Khiem et al.: Impact of Climate Change on Intensity-Duration-Frequency Curves in Ho Chi Minh City, *Journal of Climate Change Science*, 2017.
- Kim, D., Sun, Y., Wendi, D., Jiang, Z., Liang, S.-Y., and Gourbesville, P.: Flood Modelling Framework for Kuching City, Malaysia: Overcoming the Lack of Data, *Advances in Hydroinformatics*, Springer Singapore, 559–568, 559–568, https://doi.org/10.1007/978-981-10-7218-5_39, 2018.
- 635 Kim, D.-E., Gourbesville, P., and Liang, S.-Y.: Overcoming data scarcity in flood hazard assessment using remote sensing and artificial neural network, *Smart Water*, 4, <https://doi.org/10.1186/s40713-018-0014-5>, 2019.
- Koks, E. E., Bočkarjova, M., Moel, H. de, and Aerts, J. C. J. H.: Integrated Direct and Indirect Flood Risk Modeling: Development and Sensitivity Analysis, *Risk analysis an official publication of the Society for Risk Analysis*, 35, 882–900, <https://doi.org/10.1111/risa.12300>, 2015.
- 640 Kontgis, C., Schneider, A., Fox, J., Saksena, S., Spencer, J. H., and Castrence, M.: Monitoring peri-urbanization in the greater Ho Chi Minh City metropolitan area, *Applied Geography*, 53, 377–388, <https://doi.org/10.1016/j.apgeog.2014.06.029>, 2014.
- Kreibich, H., Piroth, K., Seifert, I., Maiwald, H., Kunert, U., Schwarz, J., Merz, B., and Thielen, A. H.: Is flow velocity a significant parameter in flood damage modelling?, *Nat. Hazards Earth Syst. Sci.*, 9, 1679–1692, <https://doi.org/10.5194/nhess-9-1679-2009>, 2009.
- 645 Kulp, S. A. and Strauss, B. H.: New elevation data triple estimates of global vulnerability to sea-level rise and coastal flooding, *Nature communications*, 10, 4844, <https://doi.org/10.1038/s41467-019-12808-z>, 2019.
- Kulp, S. A. and Strauss, B. H.: CoastalDEM: A global coastal digital elevation model improved from SRTM using a neural network, *Remote Sensing of Environment*, 206, 231–239, <https://doi.org/10.1016/j.rse.2017.12.026>, 2018.
- 650 LaLonde, T., Shortridge, A., and Messina, J.: The Influence of Land Cover on Shuttle Radar Topography Mission (SRTM) Elevations in Low-relief Areas, *Transactions in GIS*, 14, 461–479, <https://doi.org/10.1111/j.1467-9671.2010.01217.x>, 2010.



- Lindsay, J. B.: Efficient hybrid breaching-filling sink removal methods for flow path enforcement in digital elevation
655 models, *Hydrol. Process.*, 30, 846–857, <https://doi.org/10.1002/hyp.10648>, 2016.
- Liu, J., Shao, W., Xiang, C., Mei, C., and Li, Z.: Uncertainties of urban flood modeling: Influence of parameters for different
underlying surfaces, *Environmental Research*, 182, 108929, <https://doi.org/10.1016/j.envres.2019.108929>, 2020.
- Liu, L., Liu, Y., Wang, X., Yu, D., Liu, K., Huang, H., and Hu, G.: Developing an effective 2-D urban flood inundation
660 model for city emergency management based on cellular automata, *Nat. Hazards Earth Syst. Sci.*, 15, 381–391,
<https://doi.org/10.5194/nhess-15-381-2015>, 2015.
- Loc, H. H., Babel, M. S., Weesakul, S., Irvine, K., and Duyen, P.: Exploratory Assessment of SUDS Feasibility in Nhieu
Loc-Thi Nghe Basin, Ho Chi Minh City, Vietnam, *British Journal of Environmental & Climate Change*, 5, 2015.
- Meesuk, V., Vojinovic, Z., Mynett, A. E., and Abdullah, A. F.: Urban flood modelling combining top-view LiDAR data with
665 ground-view SfM observations, *Advances in Water Resources*, 75, 105–117,
<https://doi.org/10.1016/j.advwatres.2014.11.008>, 2015.
- Mehta, D. J., Eslamian, S., and Prajapati, K.: Flood modelling for a data-scare semi-arid region using 1-D hydrodynamic
model: a case study of Navsari Region, *Model. Earth Syst. Environ.*, 8, 2675–2685, <https://doi.org/10.1007/s40808-021-01259-5>, 2022.
- Menabde, M., Seed, A., and Pegram, G.: A simple scaling model for extreme rainfall, *Water Resour. Res.*, 35, 335–339,
670 <https://doi.org/10.1029/1998WR900012>, 1999.
- Miedema, F.: *Open Science: the Very Idea*, Springer Netherlands, Dordrecht, 2022.
- Minh Nhat et al.: Establishment of Intensity-Duration-Frequency Curves for Precipitation in the Monsoon Area of Vietnam,
Annals of Disas. Prev. Res. Inst., 93–103, 2006.
- Molinari, D., Menoni, S., Aronica, G. T., Ballio, F., Berni, N., Pandolfo, C., Stelluti, M., and Minucci, G.: Ex post damage
675 assessment: an Italian experience, *Nat. Hazards Earth Syst. Sci.*, 14, 901–916, <https://doi.org/10.5194/nhess-14-901-2014>, 2014.
- Mons, B., Neylon, C., Velterop, J., Dumontier, M., Da Silva Santos, L. O. B., and Wilkinson, M. D.: Cloudy, increasingly
FAIR; revisiting the FAIR Data guiding principles for the European Open Science Cloud, *ISU*, 37, 49–56,
<https://doi.org/10.3233/ISU-170824>, 2017.
- 680 Moy de Vitry, M., Kramer, S., Wegner, J. D., and Leitão, J. P.: Scalable flood level trend monitoring with surveillance
cameras using a deep convolutional neural network, *Hydrol. Earth Syst. Sci.*, 23, 4621–4634,
<https://doi.org/10.5194/hess-23-4621-2019>, 2019.
- Muhadi, N. A., Abdullah, A. F., Bejo, S. K., Mahadi, M. R., and Mijic, A.: Deep Learning Semantic Segmentation for Water
Level Estimation Using Surveillance Camera, *Applied Sciences*, 11, 9691, <https://doi.org/10.3390/app11209691>, 2021.
- 685 NASA/METI/AIST/Japan Spacesystems and U.S./Japan ASTER Science Team: ASTER Global Digital Elevation Model
V003, 2019.



- Neal, J., Schumann, G., and Bates, P.: A subgrid channel model for simulating river hydraulics and floodplain inundation over large and data sparse areas, *Water Resour. Res.*, 48, <https://doi.org/10.1029/2012WR012514>, 2012.
- 690 Nizam Ismail, M. S.: A STUDY ON THE EFFECT OF FLOODING DEPTHS AND DURATION ON SOIL SUBGRADE PERFORMANCE AND STABILITY, *GEOMATE*, 19, <https://doi.org/10.21660/2020.71.9336>, 2020.
- Nkwunonwo, U. C., Whitworth, M., and Baily, B.: A review of the current status of flood modelling for urban flood risk management in the developing countries, *Scientific African*, 7, e00269, <https://doi.org/10.1016/j.sciaf.2020.e00269>, 2020.
- NOAA: Climate Data Online, <https://www.ncdc.noaa.gov/cdo-web/>, last access: 14 September 2022, 2022.
- 695 O’Hara, R., Green, S., and McCarthy, T.: The agricultural impact of the 2015–2016 floods in Ireland as mapped through Sentinel 1 satellite imagery, *Irish Journal of Agricultural and Food Research*, 58, 44–65, <https://doi.org/10.2478/ijaf-2019-0006>, 2019.
- OpenTopography: ALOS World 3D - 30m, 2016.
- Ozdemir, H., Sampson, C. C., Almeida, G. A. M. de, and Bates, P. D.: Evaluating scale and roughness effects in urban flood modelling using terrestrial LIDAR data, *Hydrology and Earth System Sciences*, 17, 4015–4030, <https://doi.org/10.5194/hess-17-4015-2013>, available at: <https://hess.copernicus.org/articles/17/4015/2013/>, 2013.
- 700 Pandya, U., Patel, D. P., and Singh, S. K.: A flood assessment of data scarce region using an open-source 2D hydrodynamic modeling and Google Earth Image: a case of Sabarmati flood, India, *Arab J Geosci*, 14, <https://doi.org/10.1007/s12517-021-08504-2>, 2021.
- 705 Patro, S., Chatterjee, C., Singh, R., and Raghuwanshi, N. S.: Hydrodynamic modelling of a large flood-prone river system in India with limited data, *Hydrol. Process.*, 23, 2774–2791, <https://doi.org/10.1002/hyp.7375>, 2009.
- Phung, P.: Climate change adaptation planning under uncertainty in Ho Chi Minh City, Vietnam: a case study on institutional vulnerability, adaptive capacity and climate change governance, PhD, Planning and Stransport, University of Westminster, Westminster, 2016.
- 710 Planet Observer: PlanetDEM 30 Plus, 2017.
- Quan, N. H., Hieu, N. D., van Thu, T. T., Buchanan, M., Canh, N. D., da Cunha Oliveira Santos, M., Luan, P. D. M. H., Hoang, T. T., Phung, H. L. T., Canh, K. M., and Smith, M.: Green Infrastructure Modelling for Assessment of Urban Flood Reduction in Ho Chi Minh city, in: *CIGOS 2019, Innovation for Sustainable Infrastructure*, edited by: Ha-Minh, C., van Dao, D., Benboudjema, F., Derrible, S., Huynh, D. V. K., and Tang, A. M., Springer Singapore, Singapore, 715 1105–1110, https://doi.org/10.1007/978-981-15-0802-8_177, 2020.
- Quan et al.: Xây dựng đường cong IDF mưa cực đoan cho trạm Tân Sơn Hòa giai đoạn 1980 – 2015, *TẠP CHÍ PHÁT TRIỂN KHOA HỌC VÀ CÔNG NGHỆ*, 2017.
- Rättich, M., Martinis, S., and Wieland, M.: Automatic Flood Duration Estimation Based on Multi-Sensor Satellite Data, *Remote Sensing*, 12, 643, <https://doi.org/10.3390/rs12040643>, 2020.



- 720 René, J.-R., Djordjević, S., Butler, D., Madsen, H., and Mark, O.: Assessing the potential for real-time urban flood forecasting based on a worldwide survey on data availability, *Urban Water Journal*, 11, 573–583, <https://doi.org/10.1080/1573062X.2013.795237>, 2014.
- Rexer, M. and Hirt, C.: Comparison of free high resolution digital elevation data sets (ASTER GDEM2, SRTM v2.1/v4.1) and validation against accurate heights from the Australian National Gravity Database, *Australian Journal of Earth Sciences*, 61, 213–226, <https://doi.org/10.1080/08120099.2014.884983>, 2014.
- 725 SAIGON PORT JOINT STOCK COMPANY: PORT INFORMATION, SAIGON PORT JOINT STOCK COMPANY, <http://csg.com.vn/thong-tin/ha-tang-trang-thiet-bi>, last access: 07.22.2022, 2019.
- Sampson, C. C., Smith, A. M., Bates, P. D., Neal, J. C., and Trigg, M. A.: Perspectives on Open Access High Resolution Digital Elevation Models to Produce Global Flood Hazard Layers, *Front. Earth Sci.*, 3, <https://doi.org/10.3389/feart.2015.00085>, 2016.
- 730 Sandbach, S. D., Nicholas, A. P., Ashworth, P. J., Best, J. L., Keevil, C. E., Parsons, D. R., Prokocki, E. W., and Simpson, C. J.: Hydrodynamic modelling of tidal-fluvial flows in a large river estuary, *Estuarine, Coastal and Shelf Science*, 212, 176–188, <https://doi.org/10.1016/j.ecss.2018.06.023>, 2018.
- Sanders, B. F.: Evaluation of on-line DEMs for flood inundation modeling, *Advances in Water Resources*, 30, 1831–1843, <https://doi.org/10.1016/j.advwatres.2007.02.005>, 2007.
- 735 Sandink, D.: Urban flooding and ground-related homes in Canada: an overview, *Journal of Flood Risk Management*, 9, 208–223, <https://doi.org/10.1111/jfr3.12168>, 2016.
- Scheiber, L., David, G., Hoballah Jalloul, M., Visscher, J., Leitold, R., Revilla Diez, J., and Schlurmann, T.: Low-regret Climate Change Adaptation in Coastal Megacities – Evaluating Large-Scale Flood Protection and Small-Scale Rainwater Detention Measures for Ho Chi Minh City, Vietnam, In Review.
- 740 Schellekens, J., Broolsma, R. J., Dahm, R. J., Donchyts, G. V., and Winsemius, H. C.: Rapid setup of hydrological and hydraulic models using OpenStreetMap and the SRTM derived digital elevation model, *Environmental Modelling & Software*, 61, 98–105, <https://doi.org/10.1016/j.envsoft.2014.07.006>, 2014.
- Schlurmann, T., Kongko, W., Goseberg, N., Natawidjaja, D. H., and Sieh, K.: Near-field tsunami hazard map Padang, West Sumatra: Utilizing high resolution geospatial data and reasonable source scenarios, <https://doi.org/10.15488/1839>, 2010.
- 745 Schumann, G. J.-P., Bates, P. D., Neal, J. C., and Andreadis, K. M.: Technology: Fight floods on a global scale, *Nature*, 507, 169, <https://doi.org/10.1038/507169e>, 2014.
- Schumann, G. J.-P. and Bates, P. D.: The Need for a High-Accuracy, Open-Access Global DEM, *Front. Earth Sci.*, 6, <https://doi.org/10.3389/feart.2018.00225>, 2018.
- 750 Scussolini, P., van Tran, T. T., Koks, E., Diaz-Loaiza, A., Ho, P. L., and Lasage, R.: Adaptation to Sea Level Rise: A Multidisciplinary Analysis for Ho Chi Minh City, Vietnam, *Water Resour. Res.*, 53, 10841–10857, <https://doi.org/10.1002/2017WR021344>, 2017.



- Selaman, O. S., Said, S., and Ptuheha, F. J.: Flood Frequency Analysis for Sarawak Using Weibull, Grigorten And L-Moments Formula, *Journal - The Institution of Engineers, Malaysia*, 68, 43–52, 2007.
- Shortridge, A. and Messina, J.: Spatial structure and landscape associations of SRTM error, *Remote Sensing of Environment*, 115, 1576–1587, <https://doi.org/10.1016/j.rse.2011.02.017>, 2011.
- Shrestha, B. B., Okazumi, T., Miyamoto, M., and Sawano, H.: Flood damage assessment in the Pampanga river basin of the Philippines, *Journal of Flood Risk Management*, 9, 355–369, <https://doi.org/10.1111/jfr3.12174>, 2016.
- Storch, H.: Exploring the spatial-temporal linkages of climate response and rapid urban growth in Ho Chi Minh City, 47th ISOCARP Congress, 2011.
- Takaku, J. and Tadono, T.: Quality updates of ‘AW3D’ global DSM generated from ALOS PRISM, in: 2017 IEEE International Geoscience and Remote Sensing Symposium (IGARSS), Fort Worth, TX, 7/23/2017 - 7/28/2017, 5666–5669, 2017.
- Tang, J. C. S., Vongvisessomjai, S., and Sahasakmontri, K.: Estimation of flood damage cost for Bangkok, *Water Resources Management*, 6, 47–56, <https://doi.org/10.1007/BF00872187>, 1992.
- Taubenböck, H., Goseberg, N., Setiadi, N., Lämmel, G., Moder, F., Oczipka, M., Klüpfel, H., Wahl, R., Schlurmann, T., Strunz, G., Birkmann, J., Nagel, K., Siegert, F., Lehmann, F., Dech, S., Gress, A., and Klein, R.: "Last-Mile" preparation for a potential disaster – Interdisciplinary approach towards tsunami early warning and an evacuation information system for the coastal city of Padang, Indonesia, *Nat. Hazards Earth Syst. Sci.*, 9, 1509–1528, <https://doi.org/10.5194/nhess-9-1509-2009>, 2009.
- Thielen, A. H., Müller, M., Kreibich, H., and Merz, B.: Flood damage and influencing factors: New insights from the August 2002 flood in Germany, *Water Resources Res.*, 41, <https://doi.org/10.1029/2005WR004177>, 2005.
- Tighe, M. & Chamberlain, D.: Accuracy Comparison of the SRTM, ASTER, NED, NEXTMAP USA Digital Terrain Model over Several USA Study Sites DEMs, *Proceedings of the ASPRS/MAPPS 2009 Fall Conference*, 2009.
- TRAMECO: THE INFRASTRUCTURE: Wharf and mining equipment, TRAMECO, <http://www.tracomeco.com/10/66/Co-so-ha-tang.aspx>, last access: 07.22.2022, 2014.
- Tran Ngoc, T. D., Perset, M., Strady, E., Phan, T. S. H., Vachaud, G., Quertamp, F., Gratiot, and N.: Ho Chi Minh City growing with water related challenges, UNESCO, Paris, France, 2016.
- Trinh, M. X. and Molkenhain, F.: Flood hazard mapping for data-scarce and ungauged coastal river basins using advanced hydrodynamic models, high temporal-spatial resolution remote sensing precipitation data, and satellite imageries, *Nat Hazards*, 109, 441–469, <https://doi.org/10.1007/s11069-021-04843-1>, 2021.
- Vernimmen, R., Hooijer, A., and Pronk, M.: New ICESat-2 Satellite LiDAR Data Allow First Global Lowland DTM Suitable for Accurate Coastal Flood Risk Assessment, *Remote Sensing*, 12, 2827, <https://doi.org/10.3390/rs12172827>, 2020.
- Viet, V.: A Research on Developing Datasets of Meteorological and Hydrological characteristics for Flood Preventions in Ho Chi Minh City, Vietnam: Sub-Institute of Hydrometeorology and Climate Change, Ho Chi Minh City, 2008.



- Vojinovic, Z. and Tutulic, D.: On the use of 1D and coupled 1D-2D modelling approaches for assessment of flood damage in urban areas, *Urban Water Journal*, 6, 183–199, <https://doi.org/10.1080/15730620802566877>, 2009.
- 790 Wagenaar, D. J., Bruijn, K. M. de, Bouwer, L. M., and Moel, H. de: Uncertainty in flood damage estimates and its potential effect on investment decisions, *Nat. Hazards Earth Syst. Sci.*, 16, 1–14, <https://doi.org/10.5194/nhess-16-1-2016>, available at: <https://nhess.copernicus.org/articles/16/1/2016/>, 2016.
- Wagenaar, D., Jong, J. de, and Bouwer, L. M.: Data-mining for multi-variable flood damage modelling with limited data, 2017.
- 795 Wang, Y., Chen, A. S., Fu, G., Djordjević, S., Zhang, C., and Savić, D. A.: An integrated framework for high-resolution urban flood modelling considering multiple information sources and urban features, *Environmental Modelling & Software*, 107, 85–95, <https://doi.org/10.1016/j.envsoft.2018.06.010>, 2018.
- Watt, W. E., Chow, K. C. A., Hogg, W. D., and Lathem, K. W.: A 1-h urban design storm for Canada, *Can. J. Civ. Eng.*, 13, 293–300, <https://doi.org/10.1139/l86-041>, 1986.
- 800 Wilkinson, M. D., Dumontier, M., Aalbersberg, I. J. J., Appleton, G., Axton, M., Baak, A., Blomberg, N., Boiten, J.-W., Da Silva Santos, L. B., Bourne, P. E., Bouwman, J., Brookes, A. J., Clark, T., Crosas, M., Dillo, I., Dumon, O., Edmunds, S., Evelo, C. T., Finkers, R., Gonzalez-Beltran, A., Gray, A. J. G., Groth, P., Goble, C., Grethe, J. S., Heringa, J., Hoen, P. A. C. 't, Hooft, R., Kuhn, T., Kok, R., Kok, J., Lusher, S. J., Martone, M. E., Mons, A., Packer, A. L., Persson, B., Rocca-Serra, P., Roos, M., van Schaik, R., Sansone, S.-A., Schultes, E., Sengstag, T., Slater, T., Strawn, G., Swertz, M.
- 805 A., Thompson, M., van der Lei, J., van Mulligen, E., Velterop, J., Waagmeester, A., Wittenburg, P., Wolstencroft, K., Zhao, J., and Mons, B.: The FAIR Guiding Principles for scientific data management and stewardship, *Scientific data*, 3, 160018, <https://doi.org/10.1038/sdata.2016.18>, 2016.
- Yamazaki, D., O'Loughlin, F., Trigg, M. A., Miller, Z. F., Pavelsky, T. M., and Bates, P. D.: Development of the Global Width Database for Large Rivers, *Water Resour. Res.*, 50, 3467–3480, <https://doi.org/10.1002/2013WR014664>, 2014.
- 810 Yan, K., Tarpanelli, A., Balint, G., Moramarco, T., and Di Baldassarre, G.: Exploring the Potential of SRTM Topography and Radar Altimetry to Support Flood Propagation Modeling: Danube Case Study, *J. Hydrol. Eng.*, 20, 4014048, [https://doi.org/10.1061/\(ASCE\)HE.1943-5584.0001018](https://doi.org/10.1061/(ASCE)HE.1943-5584.0001018), 2015a.
- Yan, K., Di Baldassarre, G., Solomatine, D. P., and Schumann, G. J.-P.: A review of low-cost space-borne data for flood modelling: topography, flood extent and water level, *Hydrol. Process.*, 29, 3368–3387, <https://doi.org/10.1002/hyp.10449>, 2015b.
- 815 Zhao, W., Kinouchi, T., and Nguyen, H. Q.: A framework for projecting future intensity-duration-frequency (IDF) curves based on CORDEX Southeast Asia multi-model simulations: An application for two cities in Southern Vietnam, *Journal of Hydrology*, 598, 126461, <https://doi.org/10.1016/j.jhydrol.2021.126461>, 2021.